Surface meteorology and Solar Energy (SSE) Release 6.0 Methodology
Version 3.0   April 19, 2011

I. Introduction

NASA, through its' Earth science research program has long supported satellite systems and research providing data important to the study of climate and climate processes. These data include long-term estimates of meteorological quantities and surface solar energy fluxes. These satellite and model-based products have also been shown to be accurate enough to provide reliable solar and meteorological resource data over regions where surface measurements are sparse or nonexistent, and offer two unique features – the data is global and, in general, contiguous in time. These two important characteristics, however, tend to generate very large data archives which can be intimidating for commercial users, particularly new users with little experience or resources to explore these large data sets. Moreover the data products contained in the various NASA archives are often in formats that present challenges to new users. Accordingly, NASA's Earth Science Division Applied Sciences Program has provided the means to make these data available for government and public sector usage. To foster the usage of the global solar and meteorological data, NASA supported, and continues to support, the development of the Surface meteorology and Solar Energy (SSE) data sets and web portal which has been formulated specifically for photovoltaic and renewable energy system design needs. Of equal importance is the access to these data; to this end the SSE parameters are available via a user-friendly web-based portal designed based on user needs.

The original SSE data-delivery web site, intended to provide easy access to parameters needed in the renewable energy industry (e.g. solar and wind energy), was made available to the public in 1997. The solar and meteorological data contained in this first release was based on the 1993 NASA/World Climate Research Program Version 1.1 Surface Radiation Budget (SRB) science data and TOVS data from the International Satellite Cloud Climatology Project (ISCCP). This initial design approach proved to be of limited value because of the use of "traditional" scientific terminology that was not compatible with terminology/parameters used in the energy industry to design renewable energy power systems. After consultation with industry, Release 2 SSE was made public in 1999 with parameters specifically tailored to the needs of the renewable energy community. Subsequent releases of SSE - SSE-Release 3.0 in 2000, SSE-Release 4.0 in 2003, SSE-Release 5.0 in 2005, and SSE-Release 6.0 in 2008 – have continued to build upon an interactive dialog with potential customers resulting in updated parameters using the most recent NASA data as well as inclusion of new parameters that have been requested by the user community.

The Prediction Of Worldwide Energy Resource (POWER) project was initiated in 2003 both to improve subsequent releases of SSE, and to create new datasets applicable to other industries from new satellite observations and the accompanying results from forecast modeling. The POWER web interface (http://power.larc.nasa.gov) currently provides a portal to the SSE data archive, tailored for the renewable energy industry, as well as to the Sustainable Buildings Archive with parameters tailored for the sustainable buildings community, and the Agro-climatology Archive with parameters for the agricultural industry. In general, the underlying data behind the parameters used by each of these industries is the same – solar radiation, or insolation, and meteorology, including surface and air temperatures, moisture, and winds.

The purpose of this document is to describe the underlying data contained in SSE Release 6.0, and to provide additional information relative to the various industry specific parameters, their limitations, and estimated accuracies based on information available to NASA at the time of this document. The intent is to provide information that will enable new and/or long time users to make decisions concerning the suitability of the SSE data for his or her project in a particular region of the globe. And finally, it is noted this document is focused primarily on SSE Release 6.0 and parameters of interest to the renewable energy industry although the underlying solar and meteorological data for all three POWER archives are derived from common data sources.

A companion document describes the data and parameters in the POWER/Sustainable Buildings and POWER/Agroclimatology sections of the POWER archive.

(Return to Content)

II. What's New

Relative to the previous version of SSE (i.e. Release 5.1), SSE Release 6.0 has been updated in four basic ways: (1) solar and meteorological data now spans 22 years from July 1, 1983 through June 30, 2005, versus the 10 years of coverage in Release 5.1; (2) the solar radiation data is derived from an improved inversion algorithm (SRB Release 3.0) which provides an overall improvement in the estimation of the surface solar radiation of about 2.8%; (3) the temperature data and related parameters are based upon the higher spatial resolution Goddard Earth Observing System model version 4 (GEOS-4) versus GEOS-1; and (4) additional parameters of interest to the renewable energy community have been included.

The remainder of this section provides a summary of the estimated uncertainty associated with the basic solar and meteorological data (i.e. solar radiation, temperature, surface pressure, relative humidity, and wind speed) underlying the parameters available through SSE 6.0. The uncertainty estimates were derived through comparisons with ground measurements. A more detailed description of the parameters and the procedures used to estimate their uncertainties is given in the subsequent sections of this document.

II.A Validation Summary – Solar Insolation

Quality ground-measured data are generally considered more accurate than satellite-derived values. However, measurement uncertainties from calibration drift, operational uncertainties, or data gaps are often unknown or unreported for many ground site data sets. In 1989, the World Climate Research Program estimated that most routine-operation solar-radiation ground sites had "end-to-end" uncertainties from 6 to 12%. Specialized high quality research sites such as those in the Baseline Surface Radiation Network (BSRN) are estimated to be more accurate by a factor of two.

Table II-1a summarizes the results of comparing the total or global SSE solar insolation on a horizontal surface to observations from the BSRN for the time period January 1, 1992, the beginning of the BSRN observations, through June 30, 2005. Table II-1b summarizes the results

of comparing diffuse and direct solar insolation derived from the SRB horizontal insolation to BSRN observations of the corresponding solar components. Table II-1c summarizes the results of comparing solar insolation on a south facing tilted surface derived from the SRB horizontal insolation to the corresponding insolation derived from BSRN observations.

Table II-1a: Regression analysis of SSE versus BSRN 3-hourly, monthly and daily mean insolation on a horizontal surface for the time period January 1, 1992 - June 30, 2005			
Parameter	Region	Bias (%)	RMSE (%)
Monthly Mean 3-Hrly All Sky Insolation (Figure IV-3)	Global	-2.24	15.37
	60° Poleward	-9.29	38.77
	60° Equatorward	-1.57	12.85
Daily Mean All Sky Insolation (Figure IV-4)	Global	-1.58	20.57
	60° Poleward	-7.69	41.16
	60° Equatorward	-0.83	17.87
Monthly Mean All Sky Insolation (Figure IV-5)	Global	-2.22	13.94
	60° Poleward	-8.43	32.20
	60° Equatorward	-1.25	10.62
Monthly Mean Clear Sky Insolation (Figure IV-7)	Global	-2.77	4.11
	60° Poleward	n/a	n/a
	60° Equatorward	n/a	n/a
Table II-1b: Regression analysis of SSE versus BSRN monthly mean diffuse and direct normal insolation on a horizontal surface for the time period January 1, 1992 - June 30, 2005.			
Diffuse Radiation All Sky (Figure V-1)	Global	-8.49	24.04
	60° Poleward	-15.06	37.01
	60° Equatorward	-7.03	20.70
Direct Normal Radiation All sky (Figure V-2)	Global	10.94	33.25
	60° Poleward	24.72	73.82
	60° Equatorward	8.38	23.26
Diffuse Radiation Clear Sky (Figure V-3)	Global	-0.03	11.94
	60° Poleward	n/a	n/a
	60° Equatorward	n/a	n/a
Direct Normal Radiation Clear sky (Figure V-4)	Global	1.34	4.20
	60° Poleward	n/a	n/a
	60° Equatorward	n/a	n/a
Table II-1c: Regression analysis of SSE versus BSRN monthly mean insolation on a tilted surface for the time period January 1, 1992 - June 30, 2005.			
Monthly Mean All Sky Insolation (Figure VI.2)	Global	2.92	13.70
	60° Poleward	n/a	n/a
	60° Equatorward	n/a	n/a

II.B Validation Summary – Meteorology

Table II.2 summarize the results of comparing GEOS-4 meteorological parameters to ground observations from the National Climatic Data Center (NCDC). Table II.3 summarizes the comparison statistics for wind speeds. The SSE Release 6.0 wind speeds have been carried over from SSE Release 4 because newer data sets do not provide enough information about vegetation/surface types to permit an updated validation of the resulting wind data. The RETScreen Weather Database (RETScreen 2005) was used to test uncertainties in the SSE Release 4 wind speeds.

Table II-2: Linear least squares regression analysis of SSE GEOS-4 meteorological values versus NCDC monthly averaged values for the time period January 1983 through December 31, 2006					
Parameter	Slope	Intercept	R^2	RMSE	Bias
Tmax (°C)	0.99	-1.58	0.95	3.12	-1.83
Tmin (°C)	1.02	0.10	0.95	2.46	0.24
Tave (°C)	1.02	-0.78	0.96	2.13	-0.58
Tdew (°C)	0.96	-0.80	0.95	2.46	-1.07
RH (%)	0.79	12.72	0.56	9.40	-1.92
Heating Degree Days (degree days)	1.02	12.47	0.93	77.20	17.28
Cooling Degree Days (degree days)	0.86	2.36	0.92	28.90	-5.65
Atmospheric Pressure (hPa)	0.89	102.16	0.74	27.33	-10.20

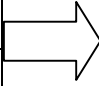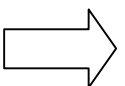| Table II-3: Estimated uncertainty for monthly averaged GEOS-1 wind speeds for the time period July 1983 through June 1993			
Parameter	Method	Bias	RMSE
Wind Speed at 10 meters for terrain similar to airports (m/s)	RETScreen Weather Database (documented 10-m height airport sites)	-0.2	1.3
	RETScreen Weather Database (unknown-height airport sites)	-0.0	1.3

(Return to Content)

III. Overview of Underlying NASA Data Used to Derive Parameters in SSE Release 6.0

SSE Release 6.0 (SSE 6.0) contains more than 200 primary and derived solar, meteorology and cloud related parameters from data spanning the 22 year period from July 1, 1983 through June 31, 2005. Table III.1 gives an overview of the various NASA programs from which the underlying solar and meteorological data are obtained and Table III.2 shows a more explicit list of the underlying data used to derive the parameters currently available through SSE 6.0. Table III.3 gives an overview list of most of the parameters available through SSE 6.0. The parameters listed in Table III.3 are available globally on a 1-degree latitude, longitude grid which is selectable by the user. Typically the value of the parameter is given in a tabular format as a monthly average over the 22-year time span July 1983 – June 2005.

The underlying solar and cloud related data (Table III.1) are obtained from the Surface Radiation Budget (SRB) portion of NASA's Global Energy and Water Cycle Experiment (GEWEX). The current SRB archive is Release 3.0 (http://eosweb.larc.nasa.gov/PRODOCS/srb/table_srb.html).

Table III-1. SSE Release 6.0 Data Flow/Sources		
Programs Contributing to SSE Release 6.0		**SSE Release 6.0**
NASA/ISCCP & CERES/MODIS: TOA Radiance, Clouds, and Surface Parameters	**NASA GEWEX/SRB Release 3.0:** Global estimates of the short and long wavelength solar radiation at earth's surface	(See Table 2 for explicit list of data from underlying projects)
NCAR MATCH: Aerosols		
TOMS/TOVS: Ozone		
NASA/GMAO GEOS-4: Atmospheric temperature and humidity profiles and surface parameters.		
NASA/GMAO GEOS-1: Winds at 1st layer above the earth's surface		
NOAA/GPCP: Surface precipitation		

The underlying meteorological data were obtained from NASA's Global Model and Assimilation Office (GMAO), Goddard Earth Observing System model version 4 (GEOS-4), and precipitation parameters were obtained from the Global Precipitation Climate Project (GPCP). The wind data is based upon the NASA/GMAO GEOS version 1 (GEOS-1).

The right most column of Table III.2 enumerates the basic parameters that are extracted from the SRB 3.0 archive, the GMAO programs (GEOS-1 & 4), and the NOAA/GPCP programs.
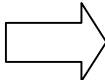
Table III-2. Basic solar and meteorological data used in SSE Release 6.0		
Contributing Programs (see Table III.1)		**SSE Archive.**
NASA GEWEX/SRB Release 3.0: Global estimates of the solar and thermal infrared wavelength radiation at earth's surface and top of atmosphere		**Daily averaged parameters (July 1, 1983 - June 30, 2005):** 1. Top of atmosphere insolation 2. Shortwave (solar, 0.2 - 4.0 µm) insolation incident on a horizontal surface at the Earth's surface 3. Longwave (thermal infrared, 4.0 - 100 µm) radiative flux incident on a horizontal surface at the Earth's surface 4. Clear sky insolation on a horizontal surface at the Earth's surface
NASA GMAO GEOS-4: Air temperatures and moisture near the surface and through the atmosphere		
NASA GMAO GEOS-1: Winds at 50m above earth's surface		**Monthly averaged parameters (July 1, 1983 - June 30, 2005):** 1. Cloud amount at available (0, 3, 6, 9, 12, 15, 18, 21) UT times 2. Frequency of cloud amount at 0, 3, 6, 9, 12, 15, 18, and 21 UT 3. Average insolation at available (0, 3, 6, 9, 12, 15, 18, 21) UT times 4. Average insolation at available (0, 3, 6, 9, 12, 15, 18, 21) UT times (Number of clear sky days (cloud amount < 10%). 5. Surface Albedo 6. Total column precipitable water 7. Minimum available insolation over consecutive-day period (1, 3, 7, 14, and 21 days) 8. Maximum available insolation over consecutive-day period (1, 3, 7, 14, and 21 days) 9. Surface precipitation (2.5°x2.5° latitude-longitude)
NOAA/GPCP: Monthly averaged surface precipitation		

Table III-3. Overview of climatologically averaged parameters in SSE Release 6.0

1. Parameters for Solar Cooking:
- Average insolation
- Midday insolation
- Clear sky insolation
- Clear sky days

2. Parameters for Sizing and Pointing of Solar Panels and for Solar Thermal Applications:
- Insolation on horizontal surface (Average, Min, Max)
- Diffuse radiation on horizontal surface (Average, Min, Max)
- Direct normal radiation (Average, Min, Max)
- Insolation at 3-hourly intervals
- Insolation clearness index, K (Average, Min, Max)
- Insolation normalized clearness index
- Clear sky insolation
- Clear sky insolation clearness index
- Clear sky insolation normalized clearness index
- Downward Longwave Radiative Flux

3. Solar Geometry:
- Solar Noon
- Daylight Hours
- Daylight average of hourly cosine solar zenith angles
- Cosine solar zenith angle at mid-time between sunrise and solar noon
- Declination
- Sunset Hour Angle
- Maximum solar angle relative to the horizon
- Hourly solar angles relative to the horizon
- Hourly solar azimuth angles

4. Parameters for Tilted Solar Panels:
- Radiation on equator-pointed tilted surfaces
- Minimum radiation for equator-pointed tilted surfaces
- Maximum radiation for equator-pointed tilted surfaces

5. Parameters for Sizing Battery or other Energy-storage Systems:
- Minimum available insolation as % of average values over consecutive-day period
- Horizontal surface deficits below expected values over consecutive-day period
- Equivalent number of NO-SUN days over consecutive-day period

6. Parameters for Sizing Surplus-product Storage Systems:
- Available surplus as % of average values over consecutive-day period

7. Diurnal Cloud Information:
- Daylight cloud amount
- Cloud amount at 3-hourly intervals
- Frequency of cloud amount at 3-hourly intervals

8. Meteorology (Temperature):
- Air Temperature at 10 m
- Daily Temperature Range at 10 m
- Cooling Degree Days above 18 °C
- Heating Degree Days below 18 °C
- Arctic Heating Degree Days below 10 °C
- Arctic Heating Degree Days below 0 °C
- Earth Skin Temperature
- Daily Mean Earth Temperature (Min, Max, Amplitude)
- Frost Days
- Dew/Frost Point Temperature at 10 m
- Air Temperature at 3-hourly intervals

9. Meteorology (Wind):
- Wind Speed at 50 m (Average, Min, Max)
- Percent of time for ranges of Wind Speed at 50 m
- Wind Speed at 50 m for 3-hourly intervals
- Wind Direction at 50 m
- Wind Direction at 50 m for 3-hourly intervals
- Wind Speed at 10 m for terrain similar to airports

Table III-3(concl'd). Overview of climatologically averaged parameters in SSE Release 6.0

10. Meteorology (Moisture, pressure):
- Relative Humidity
- Humidity Ratio (i.e. Specific Humidity)
- Surface Pressure
- Total Column Precipitable Water
- Precipitation

11. Supporting Information
- Top of Atmosphere Insolation
- Surface Albedo

While it is not the purpose of this document to discuss in detail the process by which the basic solar data (i.e. SRB Release 3.0), the meteorological data (i.e. GEOS-4), or precipitation data (GPCP) are derived, we provide herein an overview perspective on the process for each of these data sets with particular emphasis on how these data are used in SSE Release 6.0. More detailed descriptions of the SRB, GEOS-4, and GPCP data can be found in documentation and publications enumerated on their respective online web sites at http://gewex-srb.larc.nasa.gov, http://eosweb.larc.nasa.gov/PRODOCS/srb/table_srb.html, http://gmao.gsfc.nasa.gov/index.php, http://precip.gsfc.nasa.gov, and http://disc.sci.gsfc.nasa.gov/precipitation/.

(Return to Content)

IV. Global Insolation on a Horizontal Surface

The solar radiation and cloud parameters contained in SSE 6.0 are obtained directly or derived from parameters available from the NASA/Global Energy and Water Cycle Experiment - Surface Radiation Budget (NASA/GEWEX SRB) Project Release 3.0 archive (http://eosweb.larc.nasa.gov/PRODOCS/srb/table_srb.html). The NASA/GEWEX SRB Project focuses on providing estimates of the Earth's Top-of-atmosphere (TOA) and surface radiative energy flux components.

A. Earth's Radiation Budget: Figure IV.1 illustrates the major components/processes associated with the Earth's Energy Budget including the radiative flux components estimated from SRB Release 3.0 in the yellow boxes. These values are based on a 24 year (July 1983 – Dec. 2007) annual global averaged radiative fluxes with year-to-year annual average variability of +/- 4 W m^{-2} in the solar wavelengths and +/- 2 W m^{-2} in the thermal infrared (longwave) flux estimates. The absolute uncertainty of these components is still the subject of active research. For instances, the most recent satellite based measurements of the incoming solar radiation disagree with previous measurements and indicate this value should be closer 340.3 W m^{-2} providing another source of uncertainty. Other uncertainties involving the calibration of satellite radiances, atmospheric properties of clouds, aerosols and gaseous constituents, surface spectral albedos are all the subject of research within the SRB project.

Figure IV-1. The major components/processes associated with the Earth's Energy Budget. The values in the yellow rectangles are based upon the updated solar and thermal infrared radiation estimates in SRB Release 3.0. (Note that all units are in W/m^2; multiplying W/m^2 by 0.024 yields kWh/day/m^2, and by 0.0864 yields MJ/day/m^2.)
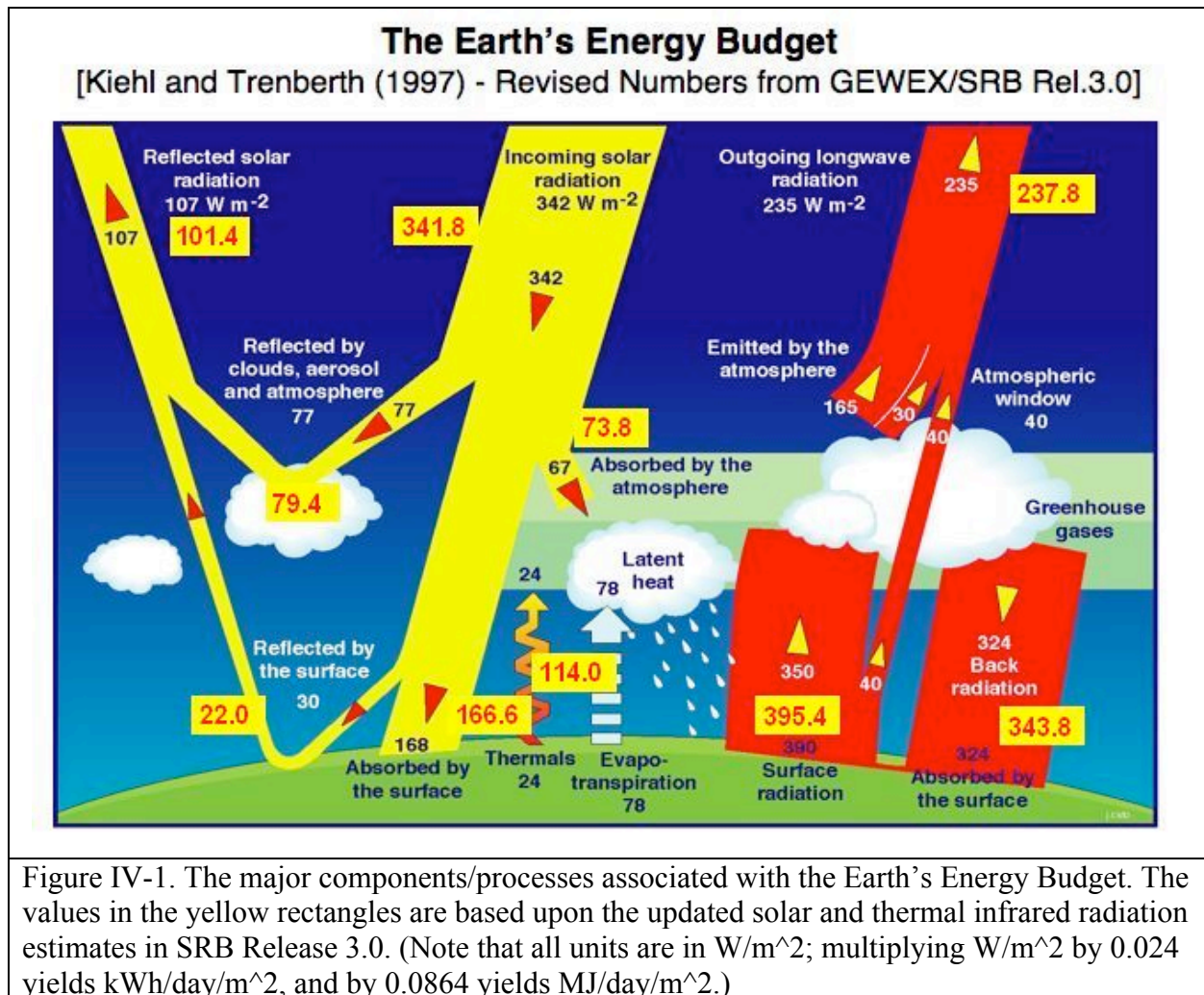
B. SRB Radiative Transfer Model: The process of inferring the surface solar radiation, or insolation, from satellite observations employs the modified method of Pinker and Laszlo (1992). This method involves the use of a radiative transfer model, along with water vapor column amounts from the GEOS-4 product and ozone column amounts from satellite measurements. Three satellite visible radiances are used: the instantaneous clear sky radiance, the instantaneous cloudy sky radiance, and the clear sky composite radiance, which is a representation of a recent dark background value. The observed satellite radiances are converted into broadband shortwave TOA albedos, using Angular Distribution Models from the Earth Radiation Budget Experiment (Smith et al., 1986). The spectral shape of the surface albedo is fixed by surface type. The radiative transfer model (through the use of lookup tables) is then used to find the absolute value of the surface albedo which produces a TOA upward flux which matches the TOA flux from the conversion of the clear-sky composite radiance. For this step, a first guess of the aerosol amount is used. The aerosol used for this purpose was derived from six years (2000-2005) of daily output from the MATCH chemical transport model (Rasch *et al.,*1997). A climatology of aerosol optical depth was developed for each of the twelve months by collecting the daily data for each grid cell, and finding the mode of the frequency distribution. The mode was used rather

than the average so as to provide a typical background value of the aerosol, rather than an average which includes much higher episodic outbreak values. The surface albedo now being fixed, the aerosol optical depth is chosen within the radiative transfer model to produce a TOA flux which matches the TOA Flux from the conversion of the instantaneous clear sky radiance. Similarly the cloud optical depth is chosen to match the TOA flux implied from the instantaneous cloudy sky radiance. With all parameters now fixed, the model outputs a range of parameters including surface and TOA fluxes. All NASA/GEWEX SRB parameters are output on a 1^0 by 1^0 global grid at 3-hourly temporal resolution for each day of the month.

Primary inputs to the model include: visible and infrared radiances, and cloud and surface properties inferred from International Satellite Cloud Climatology Project (ISCCP) pixel-level (DX) data (Rossow and Schiffer, 1999; data sets and additional information can be found at http://eosweb.larc.nasa.gov/PRODOCS/isccp/table_isccp.html); temperature and moisture profiles from GEOS-4 reanalysis product obtained from the NASA Global Modeling and Assimilation Office (GMAO; Bloom et al., 2005); and column ozone amounts constituted from Total Ozone Mapping Spectrometer (TOMS) and TIROS Operational Vertical Sounder (TOVS) archives, and Stratospheric Monitoring-group's Ozone Blended Analysis (SMOBA), an assimilation product from NOAA's Climate Prediction Center.

To facilitate access to the SRB data products, the SSE project extracts the parameters listed in Table III.2 from the SRB archive, as well as other parameters from the GEOS-4 and GPCP archives. The data products listed in Table III.2 are available through the respective archives although in some instances the product may be bundled with a number of other parameters and generally are large global spatial files (i.e. 1 per day) rather than temporal files.

C. Validation: The solar data in the SRB Release 3.0 and subsequently in SSE Release 6 have been tested/validated against research quality observation from the Baseline Surface Radiation Network (BSRN; Ohmura *et al*., 1999). Figure IV-2 shows the location of ground stations within the BSRN networks/archives. Scatter plots showing the total (i.e. diffuse plus direct) surface insolation observed at the BSRN ground sites versus insolation values from the SRB release 3.0 archive are shown in Figures IV-3 for the monthly averaged 3-hourly values, in Figure IV-4 for daily mean values, and in Figure IV-5 for monthly averaged values. Each plot covers the time period January 1, 1992, the earliest that data from BSRN is available, through June 30, 2005. We note here that 3-hourly SRB values are the initial values estimated through the retrieval process described above and are used to calculate the daily total insolation shown in Figure IV-4 and the monthly averages shown in Figure IV-5. The 3-hourly values are available through the Atmospheric Science Data Center (ASDC/SRB – http://eosweb.larc.nasa.gov/PRODOCS/srb/table_srb.html). Global spatial files of the daily and monthly insolation values are also available from ASDC/SRB. A more extensive array of parameters based upon the daily and monthly SRB data for user defined latitude-longitude coordinates is available through the SSE Release 6 web site (http://eosweb.larc.nasa.gov/PRODOCS/sse/table_sse.html)
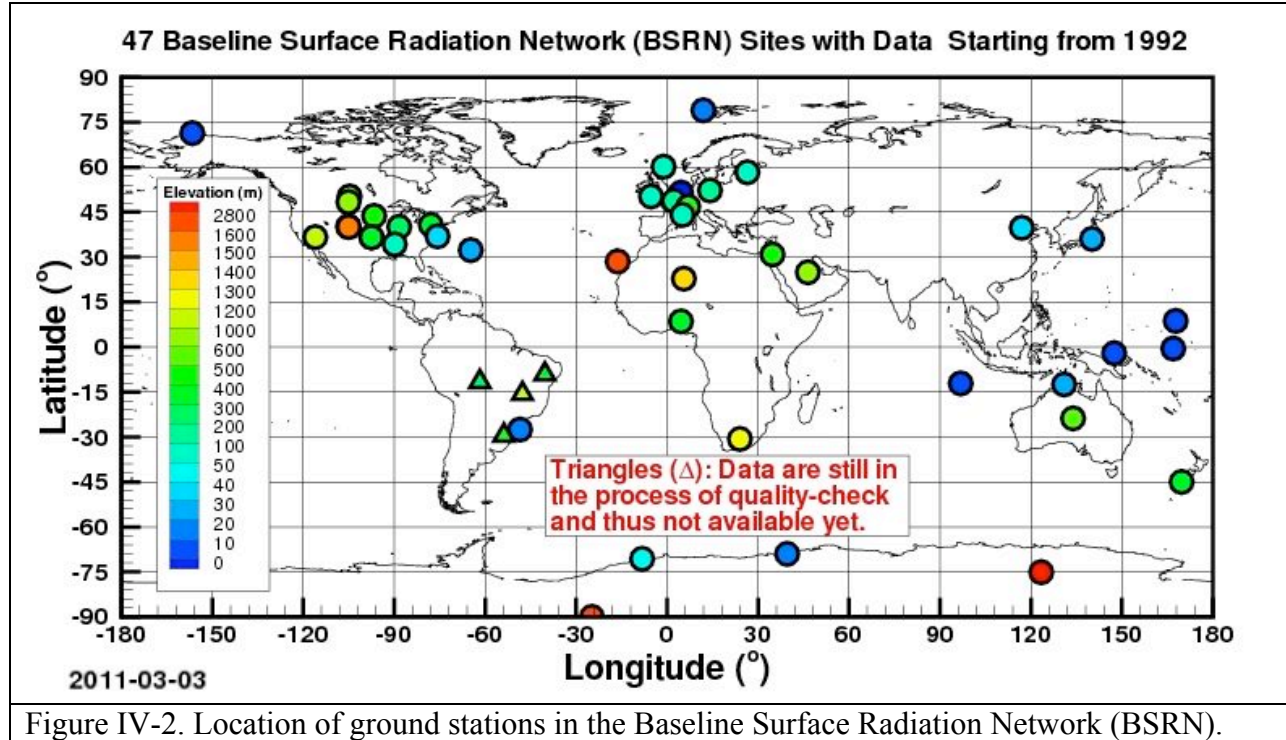
Figure IV-2. Location of ground stations in the Baseline Surface Radiation Network (BSRN).

Correlation and accuracy parameters for each scatter plots (Figures IV-3 – IV-5) are given in the legend box in each figure. Note that the correlation and accuracy parameters are given for all sites (e.g. Global), for the BSRN sites in regions above 60° latitude, north and south (i.e. 60^0 poleward), and for BSRN sites between 60° north and 60° south (i.e. 60° equatorward). The Bias is the difference between the mean (μ) of the respective solar radiation values for SRB and BSRN. The RMS is the root mean square difference between the respective SRB and BSRN values. The correlation coefficient between the SRB and BSRN values is given by ρ, the variance in the SRB values is given by σ, and N is number of SRB:BSRN pairs for each latitude region.

IV.C.i Monthly 3-Hourly Mean Insolation (All sky Conditions)

Figure IV-3. Scatter plot of 3-hourly total surface solar radiation observed at BSRN ground sites versus 3-hourly values from the SRB Release 3.0 archive. Note that solar radiation is in KWh/day/m^2; multiplying KWh/day/m^2 by 41.67 yields W/m^2, and by 3.6 yields MJ/day/m^2.)

IV.C.ii. Daily Mean Insolation (All sky Conditions)

Figure IV-4. Scatter plot of daily total surface solar radiation observed at BSRN ground sites versus daily values from the SRB Release 3.0 archive. These daily are used to calculate the monthly averages that are provided in SSE Release 6.0. (Note that solar radiation is in KWh/day/m^2; multiplying KWh/day/m^2 by 41.67 yields W/m^2, and by 3.6 yields MJ/day/m^2.)

IV.C.iii. Monthly Mean Insolation (All sky Conditions)
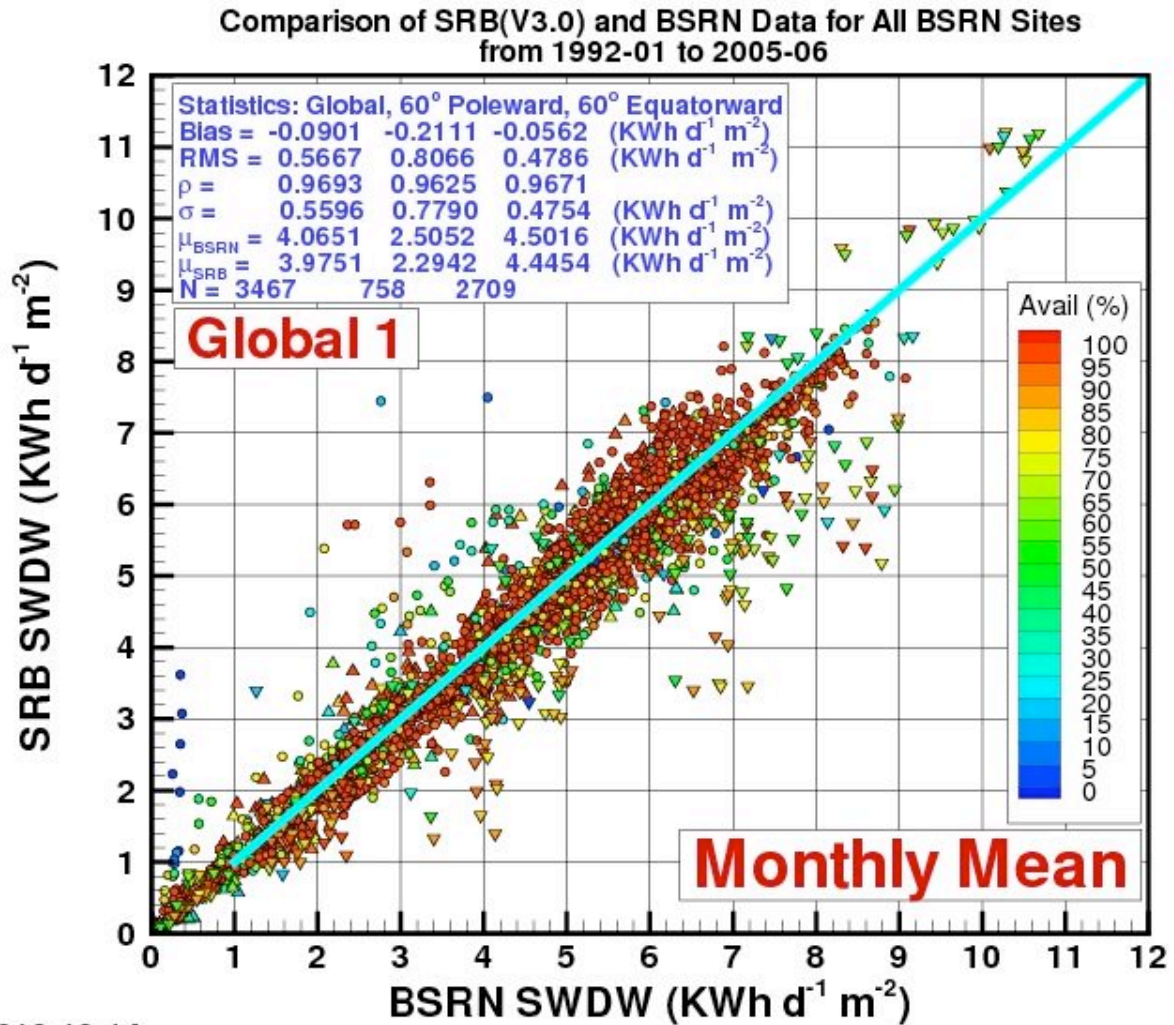
Figure IV-5. Scatter plot of monthly total surface solar radiation observed at BSRN ground sites versus monthly values from the SRB Release 3.0 archive. The daily values illustrated in figure IV-5 are used to calculate the monthly averages. The bias differs from the daily value due to differences in sampling requirements. (Note that solar radiation is in KWh/day/m^2; multiplying KWh/day/m^2 by 41.67 yields W/m^2, and by 3.6 yields MJ/day/m^2.)

IV.C.iv. Clear Sky Total: The clear sky total insolation is obtained from the SRB Release 3.0 archive. (http://eosweb.larc.nasa.gov/PRODOCS/srb/table_srb.html). In Figure IV-7 the monthly averaged total insolation on a horizontal surface is compared to ground observations from the BSRN network (Figure IV-6) for "clear" sky conditions. For these comparisons it was necessary to ensure that the ground observations and the satellite derived solar radiation values are for equivalent clear sky conditions. Fortunately, observational data from a number of BSRN ground sites (see Figure IV-6) and the satellite observational data provide information related to cloud cover for each observational period. Recall in Section III and in Table III-2, it was noted that cloud parameters from the NASA ISCCP were used to infer the solar radiation in the SRB Release 3.0 archive. Parameters within the ISCCP data provide a measure of the clearness for each satellite observation use in the SRB-inversion algorithms. Similarly, observations from upward viewing cameras at the 27 BSRN sites shown in Figure IV-6 provided a measure of cloud cover for each ground observational period. The comparison data shown in Figures IV-7 used the ground cameras and the ISCCP data to matched clearness conditions. In particular, the comparison shown below use clearness criteria defined such that clouds in the field of view of the upward viewing camera and the field of view from the ISCCP satellites must both be less than 10%.
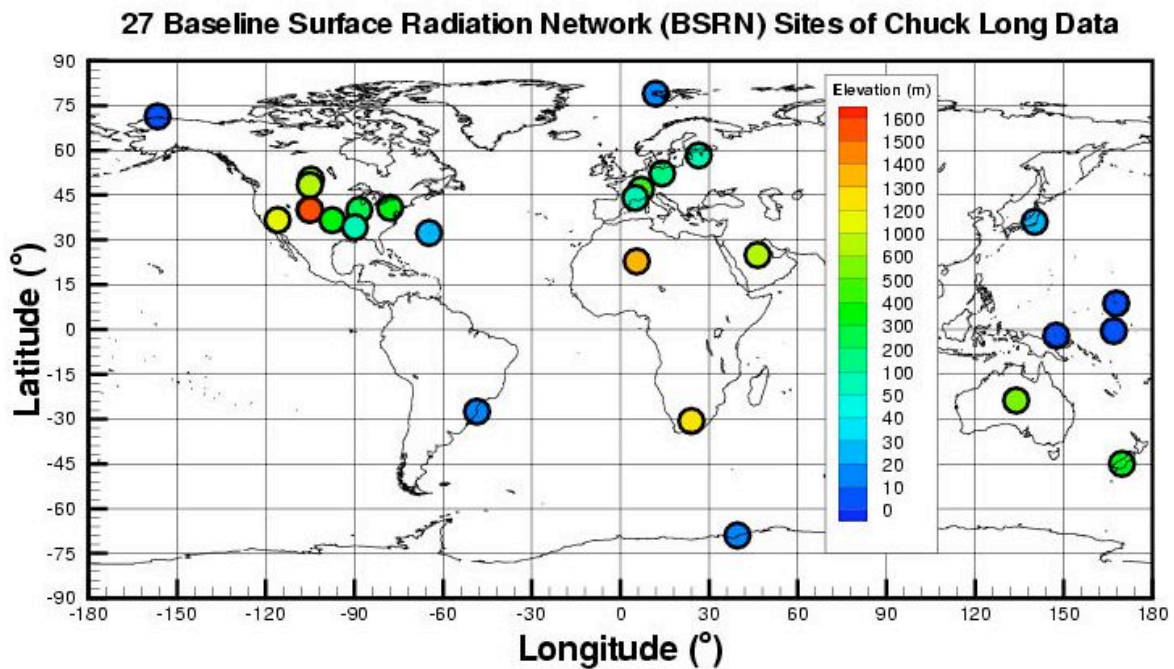
Figure IV-6. Location of ground stations in the Baseline Surface Radiation Network (BSRN) with upward viewing cameras.

Figure IV-7. Scatter plots of the monthly averaged clear sky total radiation derived from observations at BSRN ground sites vs. monthly averaged values from SRB Release 6.0. Clear sky conditions are for less than 10% cloud cover in field-of-view of both the upward viewing ground and downward viewing satellite cameras. The comparison statistics are given for the entire globe (i.e. Global), for latitudes north and south of 60^0 (i.e. 60^0 Poleward), and for latitudes from 60^0 S to 60^0 N (i.e. 60^0 Equatorward). The Bias is the difference between the mean (μ) of the respective solar radiation values for SRB and BSRN. RMS is the root mean square difference between the respective SRB and BSRN values. The correlation coefficient between the SRB and BSRN values is given by ρ, the variance in the SRB values is given by σ, and N is number of SRB:BSRN month pairs for each latitude region. (Note that the solar radiation unit is kWh/day/m^2; multiplying kWh/day/m^2 by 3.6 yields MJ/day/m^2, and by 41.67 yields W/m^2.)

V. Diffuse and Direct Normal Radiation on a Horizontal Surface

The all sky (i.e. all cloud conditions) total global solar radiation from the SRB archive discussed in Section VI is the sum of diffuse and direct normal radiation. However, estimates of all sky horizontal diffuse, $(H^{All})_{Diff}$, and direct normal radiation, $(H^{All})_{DNR}$ are often needed parameters for the design of hardware such as solar panels, solar concentrator size, day lighting, as well as agricultural and hydrology applications. From an observational perspective, $(H^{All})_{Diff}$ at the surface of the earth is that radiation remaining with $(H^{All})_{DNR}$ from the sun's beam blocked by a shadow band or tracking disk. $(H^{All})_{Diff}$ is typically measured using a sun tracking pyrheliometer with a shadow band or disk to block the direct normal radiation from the sun. Similarly, from an observational perspective, $(H^{All})_{DNR}$ is the amount of solar radiation from the direction of the sun, and is typically measured using a pyrheliometer tracking the sun through out the day.

A. SSE Method: Measurements of $(H^{All})_{Diff}$ and $(H^{All})_{DNR}$ are difficult to make and consequently are generally only available at high quality observational sites such as those in the BSRN network. In order to use the global estimates of the total surface solar radiation, H^{All} from SRB Release 3.0 to provide estimates of $(H^{All})_{Diff}$ and $(H^{All})_{DNR}$, a set of polynomial equations have been developed relating the ratio of $[(H^{All})_{Diff}]/[H^{All}]$ to the clearness index KT = $[H^{All}]/[H^{TOA}]$ using ground based observations from the BSRN network. These relationships were developed by employing observations from the BSRN network to extend the methods employed by RETScreen (RETScreen, 2005) to estimate $(H^{All})_{DNR}$.

In this section we outline the techniques for estimating the $[(H^{All})_{Diff}]$ and $[(H^{All})_{DNR}]$ from the solar insolation values available in SRB Release 3.0. In the following section results of comparative studies with ground site observations are presented, which serve to validate the resulting $[(H^{All})_{Diff}]$ and $[(H^{All})_{DNR}]$ and provide a measure of the overall accuracy of our global results.

***All Sky Monthly Averaged Diffuse Radiation* [$(H^{All})_{Diff}$]*:* As just noted, measurements of $(H^{All})_{Diff}$, $(H^{All})_{DNR}$, and H^{All} are made at the ground stations in the BSRN network. These observational data were used to develop the set of polynomial equations given below relating the ratio $[(H^{All})_{Diff}]/[H^{All}]$ to the clearness index KT = $[H^{All}]/[H^{TOA}]$. We note that the top of atmosphere solar radiation, H^{TOA}, is known from satellite observations.

For latitudes between 0 and 45 degrees North and South:
$[(H^{All})_{Diff}]/[H^{All}]$ =
    0.96268 - 1.45200*KT + 0.27365*KT^2 + (0.04279*KT^3 + 0.000246*SSHA + 0.001189*NHSA

For latitudes between 45 and 90 degrees North and South:
If SSHA = 0 - 81.4 deg:
$[(H^{All})_{Diff}]/[H^{All}]$ =1.441-(3.6839*KT)+(6.4927*KT^2)-(4.147*KT^3)+(0.0008*SSHA)-(0.008175*NHSA)

If SSHA = 81.4 - 100 deg:
$[(H^{All})_{Diff}]/[H^{All}]$ =1.6821-(2.5866*KT)+(2.373*KT^2)-(0.5294*KT^3)-(0.00277*SSHA)-

(0.004233*NHSA)

If SSHA = 100 - 125 deg:
[(H^{All})$_{Diff}$]/[H^{All}] =0.3498+(3.8035*KT)-(11.765*KT^2)+(9.1748*KT^3)+(0.001575*SSHA)-(0.002837*NHSA)

If SSHA = 125 - 150 deg:
[(H^{All})$_{Diff}$]/[H^{All}] =1.6586-(4.412*KT)+(5.8*KT^2)-(3.1223*KT^3)+(0.000144*SSHA)-(0.000829*NHSA)

If SSHA = 150 - 180 deg:
[(H^{All})$_{Diff}$]/[H^{All}] = 0.6563-(2.893*KT)+(4.594*KT^2)-(3.23*KT^3)+(0.004*SSHA)-(0.0023*NHSA)

where:
KT = [H^{All}]/[H^{TOA}]

SSHA = sunset hour angle in degrees

NHSA = noon solar angle from the horizon in degrees

The above set of polynomial equations relate the ratio of monthly averaged horizontal diffuse radiation for all sky conditions to the monthly averaged total solar radiation for all sky conditions { [(H^{All})$_{Diff}$]/[H^{All}] } to the clearness index KT = [H^{All}]/[H^{TOA}].

All Sky Monthly Averaged Direct Normal Radiation:
[(H^{All})$_{DNR}$] = ([H^{All}] - [(H^{All})$_{Diff}$])/ COS(THMT)

where:
THMT is the solar zenith angle at the mid-time between sunrise and solar noon (Gupta, et al. 2001) for the "monthly average day" (Klein 1977; also see Table VII.1 below).
COS(THMT) = f + g [(g - f)/ 2g]$^{1/2}$

H^{All} = Total of direct beam solar radiation and diffuse atmospheric radiation falling on a horizontal surface at the earth's surface
(H^{All})$_{Diff}$ = diffuse atmospheric radiation falling on a horizontal surface at the earth's surface

f = sin(latitude) sin(solar declination)

g = cos(latitude) cos(solar declination)

If the Sunset Hour Angle = 180 degrees, then COS(THMT) = f.

B. Validation: Figures V-1 and V-2 show respectively scatter plots for the monthly mean diffuse and monthly mean direct normal radiation for all sky conditions computed from measured values at the BSRN sites (designated as BSRN SWDF and BSRN SDN) versus the

corresponding SSE values (designated as SRB SWDF and SRB SWDN) derived from the expression discussed above. Figures V-3 and V-4 show similar scatter plots for clear sky conditions.

Correlation and accuracy parameters are given in the legend boxes. Note that for the all sky condition the correlation and accuracy parameters are given for all sites (e.g. Global), for the BSRN sites regions above 60^0 latitude, north and south, (i.e. 60^0 poleward) and for BSRN sites below 60^0 latitude, north and south (60^0 equatorward).

V.B.i. Monthly Mean Diffuse (All Sky Conditions)

Figure V-1. Scatter plot of the all sky monthly mean horizontal diffuse radiation calculated from BSRN observations and the corresponding radiation derived from SRB-Release 3.0 data. (Note that solar radiation is in KWh/day/m^2; multiplying KWh/day/m^2 by 41.67 yields W/m^2, and by 3.6 yields MJ/day/m^2.)
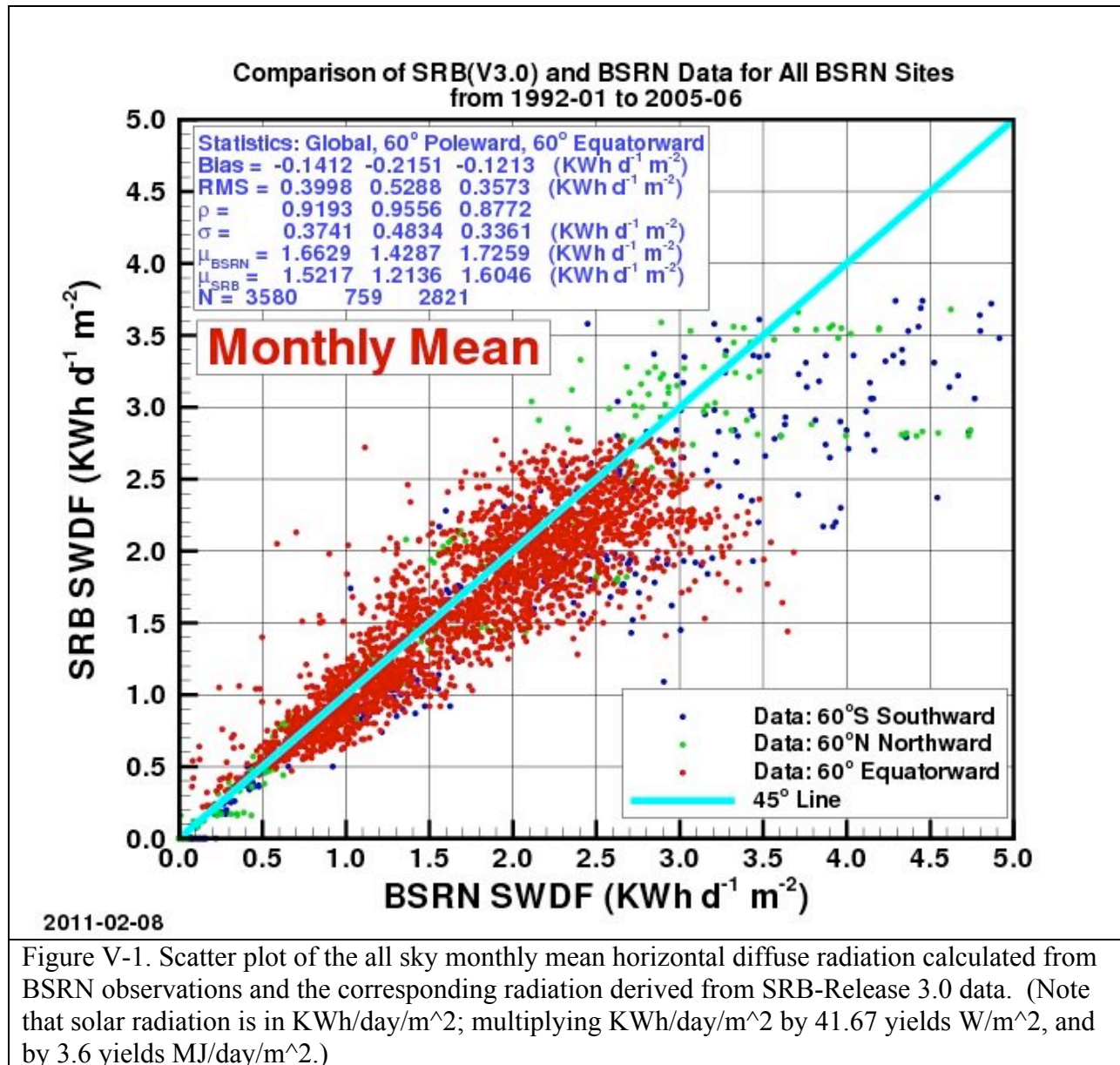
However, because of the scarcity of clear sky values only the global region is used for the statistics in Figures V-3 and V-4. The Bias is the difference between the mean (μ) of the respective solar radiation values for SRB and BSRN. RMS is the root mean square difference between the respective SRB and BSRN values. The correlation coefficient between the SRB and BSRN values is given by ρ, the variance in the SRB values is given by σ, and N is number of SRB:BSRN pairs for each latitude region.

V.B.ii. Monthly Mean Direct Normal (All Sly Conditions)

Figure V-2 compares the monthly averaged direct normal radiation for all sky conditions computed from BSRN ground observations (designated as BSRN SWDN) to monthly averaged $(H^{All})_{DNR}$ calculated from SRB-R 3.0 (designated as SRB SWDN in Figure V-2) using the expressions discussed above.
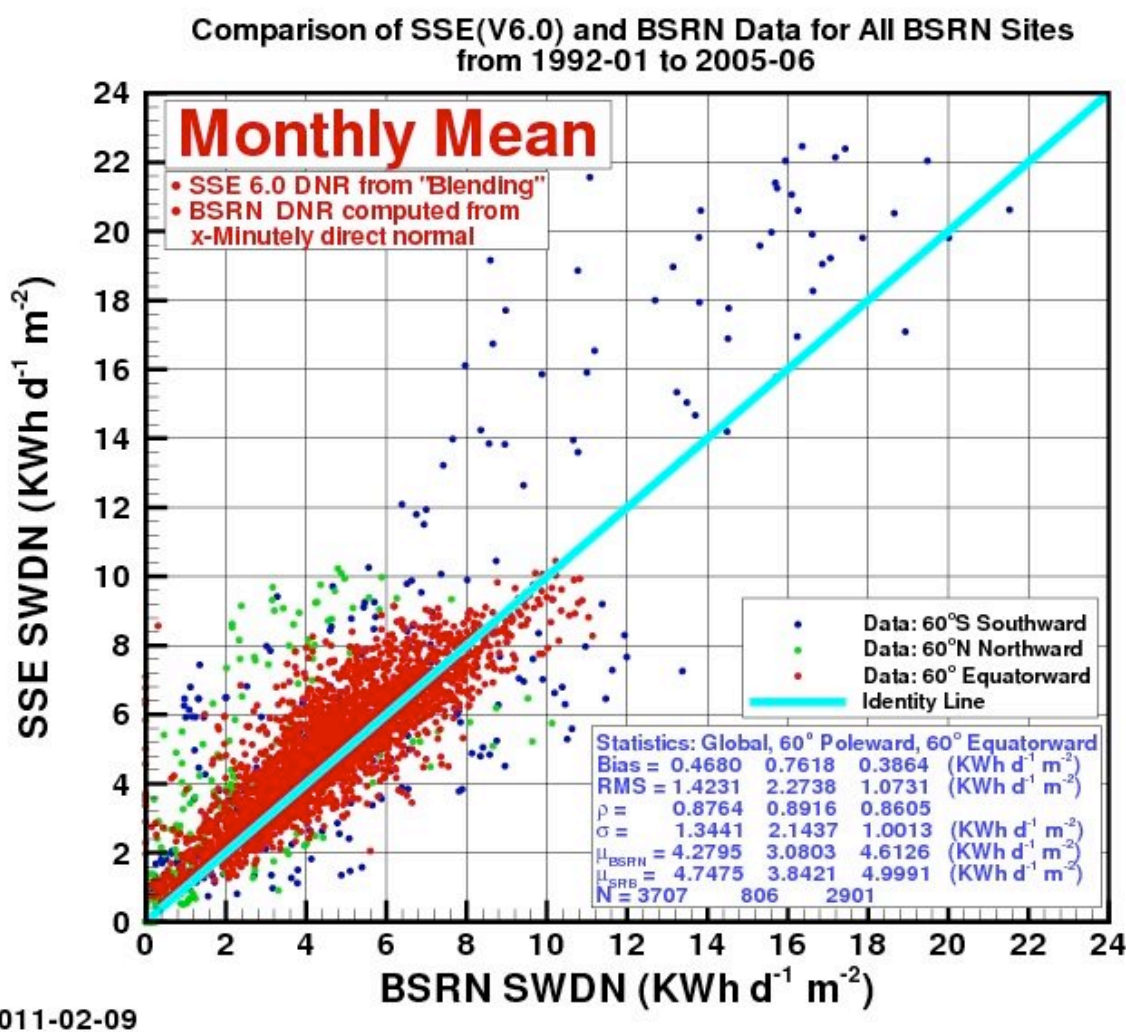
Figure V-2. Scatter plot of the monthly mean all sky direct normal radiation determined from BSRN ground observations and the corresponding radiation derived from SRB-Release 3.0 data. (Note that solar radiation is in KWh/day/m^2; multiplying KWh/day/m^2 by 41.67 yields W/m^2, and by 3.6 yields MJ/day/m^2.)

V.B.iii. Monthly Mean Diffuse (Clear Sky Conditions)
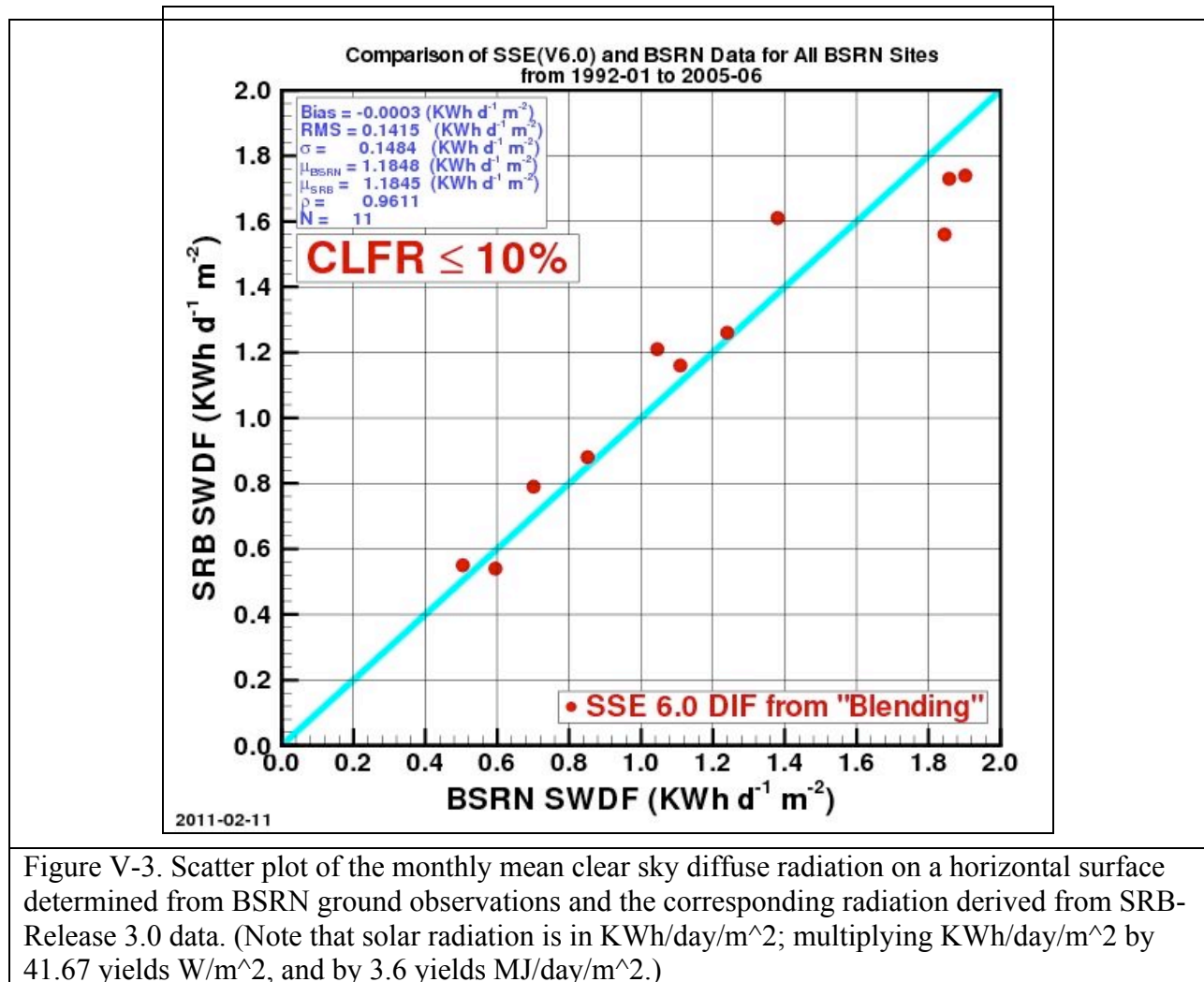
Figure V-3. Scatter plot of the monthly mean clear sky diffuse radiation on a horizontal surface determined from BSRN ground observations and the corresponding radiation derived from SRB-Release 3.0 data. (Note that solar radiation is in KWh/day/m^2; multiplying KWh/day/m^2 by 41.67 yields W/m^2, and by 3.6 yields MJ/day/m^2.)

V.B. iv. Monthly Mean Direct Normal (Clear Sky Conditions)
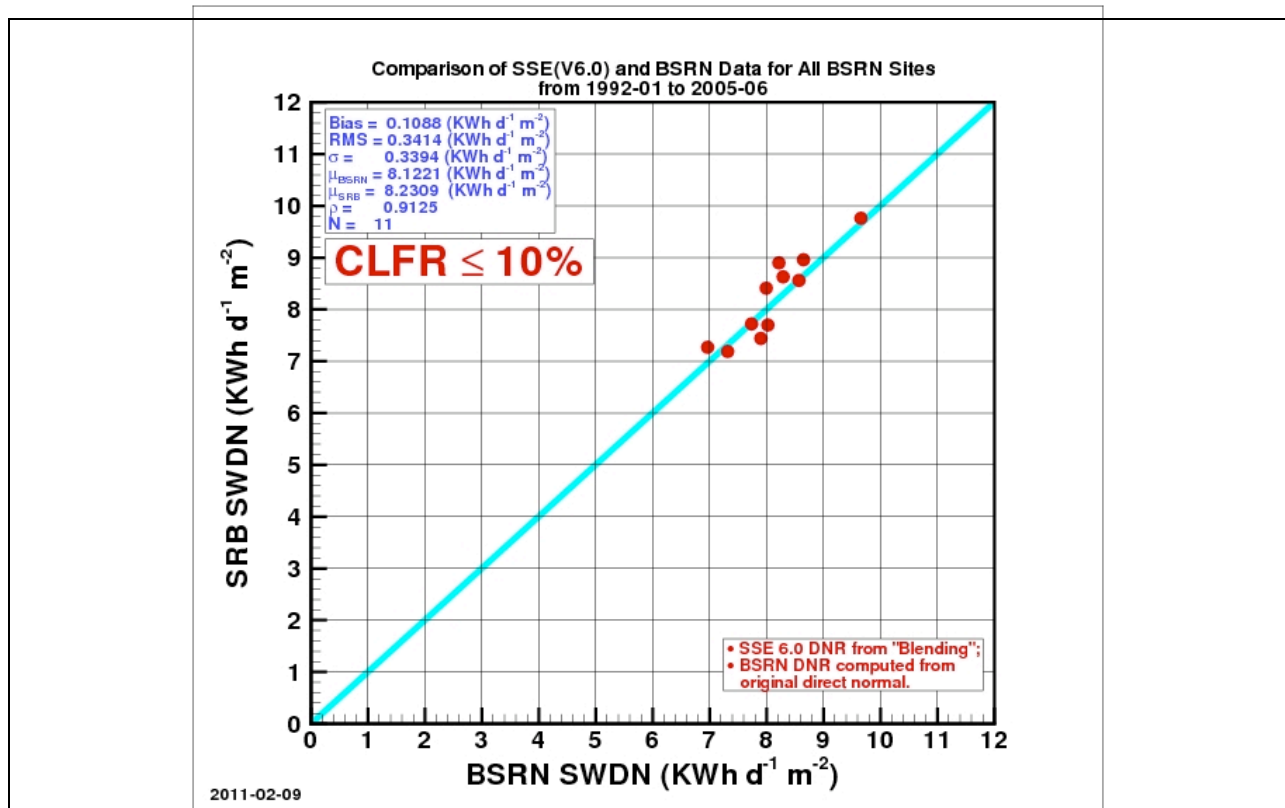
Figure V-4. Scatter plot of the monthly mean clear sky direct normal radiation on a horizontal surface determined from BSRN ground observations and the corresponding monthly mean clear sky direct normal radiation derived from SRB-Release 3.0 data. (Note that solar radiation is in KWh/day/m^2; multiplying KWh/day/m^2 by 41.67 yields W/m^2, and by 3.6 yields MJ/day/m^2.)

VI. Insolation On a Tilted Surface

The calculation of the insolation impinging on a tilted surface in SSE Release 6.0 basically follows the method employed by RETScreen (RETScreen 2005). The major difference is that the diffuse radiation is derived from the equations described in Section V which describes slight modifications on the RETScreen approach.

VI.A. Overview of RETScreen Method: In this section we briefly outline the RETScreen method. The RETScreen method uses the "monthly average day" hourly calculation procedures where the equations developed by Collares-Pereira and Rabl (1979) and Liu and Jordan (1960) are used respectively for the "monthly average day" hourly insolation and the "monthly average day" hourly diffuse radiation.

Hourly Total and Diffuse Insolation on a Horizontal Surface: We first describe the method of estimating the hourly horizontal surface insolation (H_h) and horizontal diffuse (H_{dh}) for daylight hours between 30 minutes after sunrise to 30 minutes before sunset during the "monthly average day". The "monthly average day" is the day in the month whose declination is closest to the average declination for that month (Klein 1977). Table VII.1 lists the date and average declination for each month.

Table VI.1. List of the day in the month whose solar declination is closest to the average declination for that month					
Month	Date in month	Declination	Month	Date in month	Declination
January	17	-20.9	July	17	21.2
February	16	-13.0	August	16	13.5
March	16	-2.4	September	15	2.2
April	15	9.4	October	15	-9.6
May	15	18.8	November	14	-18.9
June	11	23.1	December	10	-23.0

$$H_h = r_t H$$

$$H_{dh} = r_d H_d$$

where:

      H is the monthly average horizontal surface insolation from the SRB 3.0 data set.
      H_d is the monthly average horizontal diffuse from the method described in section V.
      $r_t = (\pi/24)*(A + B\cos\omega)*[(\cos\omega - \cos\omega_s)/(\sin\omega_s - \omega_s \cos\omega_s)]$
      (Collares-Pereira and Rabl; 1979)
      $r_d = (\pi/24)*[(\cos\omega - \cos\omega_s)/(\sin\omega_s - \omega_s \cos\omega_s)]$ (Liu and Jordan; 1960)

where:

      $A = 0.409 + 0.5016 \sin[\omega_s - (\pi/3)]$
      $B = 0.6609 - 0.4767 \sin[\omega_s - (\pi/3)]$

where:

      ω = solar hour angle for each daylight hour relative to solar noon between sunrise plus 30 minutes and sunset minus 30 minutes. The sun is displaced 15° from the local meridian for each hour from local solar noon.
      ω_s = sunset hour angle
      $\omega_s = \cos^{-1}[$-tan (solar declination)*tan(latitude)$]$, (+ = west relative to solar noon)

where:

      solar declination = $23.45*\sin[6.303*\{(284 + n)/365\}]$
      n = day number of year, 1 = January 1

Hourly total radiation on a tilted surface: Next, we describe the method of estimating hourly total radiation on a tilted surface (H_{th}) as outlined in the RETScreen tilted surface method. The equation, in general terms, is:

H_{th} = solar beam component + sky diffuse component + surface/sky reflectance component

The solution is as follows:

$\cos\theta_{zh}$ = cos(latitude) cos(solar declination) $\cos\omega$ + sin(latitude) sin(solar declination)

$\cos\theta_h = \cos\theta_{zh} \cos\beta_h + (1 - \cos\theta_{zh})(1 - \cos\beta_h)(\cos(\gamma_{sh} - \gamma_h))$

where:

β_h = hourly slope of the PV array relative to a horizontal surface. β_h is constant for fixed panels or panels in a vertical- axis tracking system. $\beta_h = \theta_z$ for panels in a two-axis tracking system. Values for other types of tracking systems are given in Braun and Mitchell (1983).

$\gamma_{sh} = \sin^{-1}[(\sin\omega \cos(\text{solar declination}))/\sin\theta_{zh}]$
= hourly solar azimuth angle; angle between the line of sight of the Sun into the horizontal surface and the local meridian. Azimuth is zero facing the equator, positive west, and negative east.

γ_h = hourly surface azimuth of the tilted surface; angle between the projection of the normal to the surface into the horizontal surface and the local meridian. Azimuth is zero facing the equator, positive west, and negative east. γ_h is constant for fixed surfaces. $\gamma_h = \gamma_{sh}$ for both vertical- and two-axis tracking systems. See Braun and Mitchell (1983) for other types of tracking systems.

$H_{th} = (H_h - H_{dh})(\cos\theta_h/\cos\theta_{zh}) + H_{dh}[(1+\cos\beta_h)/2] + H_h*\rho_s[(1-\cos\beta_h)/2]$

where:
ρ_s = surface reflectance or albedo is assumed to be 0.2 if temperature is above 0°C or 0.7 if temperature is below -5°C. Linear interpolation is used for temperatures between these values.

Finally, the monthly average tilted surface insolation (H_t) is estimated by summing hourly values of H_{th} over the "monthly average day". It was recognized that such a procedure would be less accurate than using quality "day-by-day" site measurements, but RETScreen validation studies indicate that the "monthly average day" hourly calculation procedures give tilted surface results ranging within 3.9% to 8.9% of "day-by-day" hourly methods.

For any user specified latitude and longitude, the insolation incident on an equator facing panel is provide for a horizontal panel (tilt angle = 0°), and at angles equal to the latitude, and latitude ± 15 ° along with the optimum tilt angle for the given latitude/longitude. It should be emphasized that the optimum tilt angle of a solar panel at a given latitude and longitude is not simply based on solar geometry and the site latitude. The solar geometry relative to the Sun slowly changes over the period of a month because of the tilted axis of the Earth. There is also a small change in the distance from the Sun to Earth over the month because of the elliptical Earth orbit around the Sun. The distance variation may cause a change in the trend of the weather at the latitude/longitude location of the tilted solar panel. The weather trend over the month may be
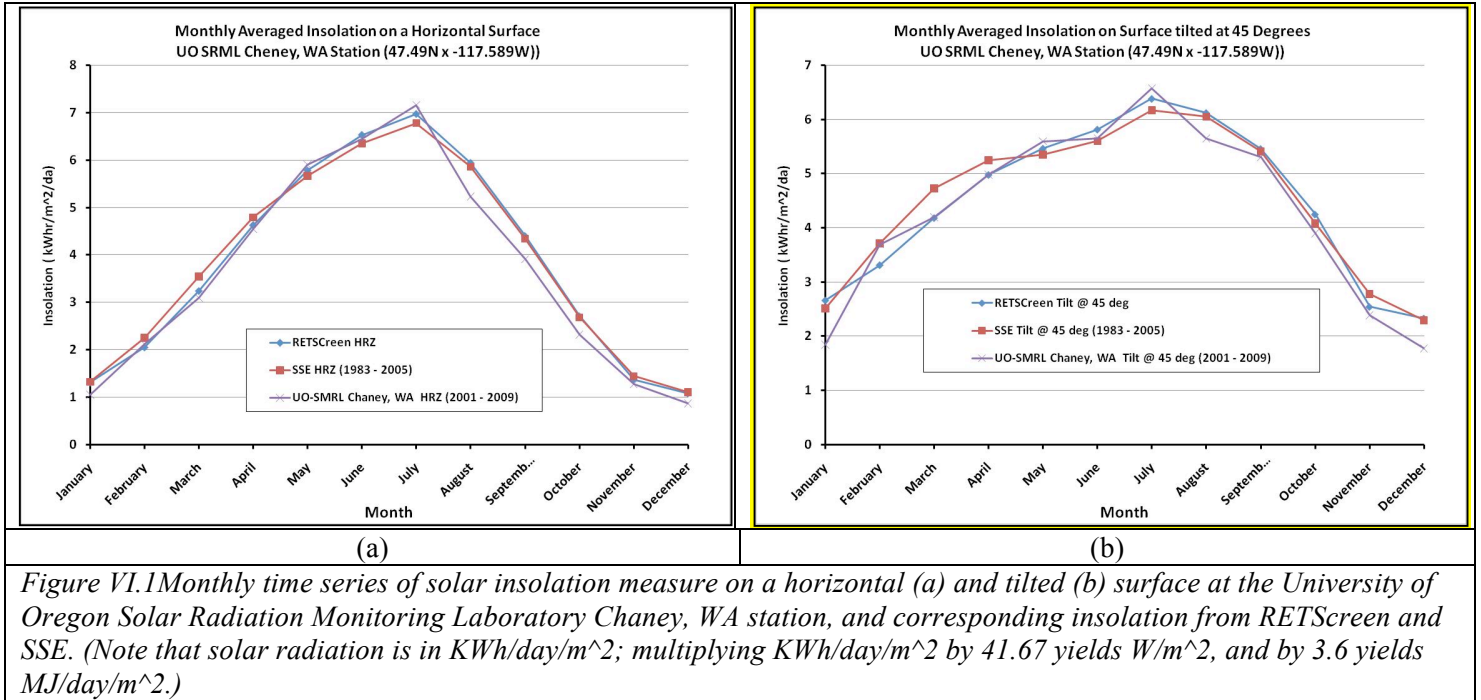
toward either clearer or more cloudy skies over that month for that particular year. Either cloudy-diffuse or clear-sky direct normal radiation may vary from year to year. As a result, the SSE project makes hourly calculations of tilted solar panel performance for a monthly-average day for all 1-degree cells over the globe for a 22-year period. Both the tilt angles and insolation values provided should be considered as average values over that 22-year period.

VI.B Validation of Monthly Mean Insolation on a Tilted Surface: In this section results from three approaches for validation of the SSE monthly mean insolation on a tilted surface are presented. The first involves comparison of the tilted surface insolation values from the SSE and RETScreen formulation. The remaining two approaches provide more definitive validation statistics in that the SSE tilted surface insolation values are compared to measured tilted surface insolation values and to values that were derived from measurements of the diffuse and direct normal components of the tilted surface radiation at BSRN sites.

VI.B i. SSE vs RETScreen. Table VI-2 summarizes the agreement between the SSE and RETScreen formulation in terms of the Bias and RMSE between the two methods, and the parameters (i.e. slope, intercept, and R^2) characterizing the linear least square fit to the RETScreen values (x-axis) to SSE Release 6.0 values (y-axis) when both the RETScreen and SSE methods have the same horizontal insolation as inputs. Recall that the major difference between the two methods involves the determination of the diffuse radiation, and note that the results from the two methods are in good agreement.

Table VI-2 Summary results from a comparison of the insolation on a tilted surface calculated by RETScreen and SSE Release 6.0 using the same monthly averaged insolation on a horizontal surface

Location	Lat x Long	Tilt Angle	Titled-Bias	Titled-RMSE	Titled-Slope	Titled-In'cept	Titled-R2
Ottawa Int'l Airport, Ontario. Canada	45.3N x 75.7W	45	0.47	0.56	1.17	-1.19	0.94
Berverlodge,Alberta,CN	55.2N x 119.4W	40	0.30	0.36	1.09	-0.65	0.99
Castlegar AP, British Cl, CN	49.3N x 117.6W	49	0.35	0.45	1.24	-1.43	0.99
Totonto Int'l AP, Ontario, CN	43.7N x 79.6W	43	0.06	0.09	1.02	-0.12	1.00
Burmingham,AL	33.6N x 86.8W	48	0.06	0.07	1.05	-0.29	1.00
Dodge City, KS	37.8N x 100.0W	37	0.04	0.07	1.01	-0.11	0.99
Covington, KY	39.1N x 84.7W	39	0.03	0.05	1.00	-0.03	1.00
San Francisco, CA	37.6N x 122.4W	37	0.03	0.05	1.00	-0.01	1.00
San Jose, Costa Rica	10.0N x 84.2W	25	-0.09	0.24	0.79	1.08	0.93
Boulogne Sur Seine, France	50.7N x 1.6E	35	0.15	0.18	1.06	-0.36	1.00
Riyadh (Saud-AFB), Saudi Arabia	24.7N x 46.7E	39	0.09	0.11	1.07	-0.51	0.99
Tabuk (Saud-AFB),Saudi Arabia	28.4N x 36.6E	43	0.07	0.09	1.09	-0.59	0.97
Bisha (Civ/Mil),Saudi Arabia	20.0N x 42.6E	35	-0.16	0.45	0.53	2.99	0.26
Beer-Sheva/Teyman,Israel	31.2N x 34.8E	46	0.05	0.09	0.98	0.07	0.99
Jerusalem/Atarot, Israel	31.5N x 35.2E	46	0.10	0.12	0.99	-0.05	0.99
Naha (Civ/JASDF), Japan	26.2N x 127.7E	41	0.07	0.08	1.00	-0.08	1.00
Brasila, Brasil	15.8S x 47.9W	30	-0.09	0.24	0.83	1.02	0.94
Antofagasta, Chile	23.4S x 70.5W	38	0.08	0.10	1.01	-0.13	1.00
Arica/Chacallute, Chile	18.4S x 70.5W	33	-0.20	0.49	1.14	-0.50	0.90
Windhoek/Eros (SAAF), Namibia	22.6S x 17.1E	37	-0.05	0.32	0.89	0.74	0.74
Pretoria (Met), S. Africa	25.7S x 28.2E	40	0.06	0.09	1.02	-0.19	0.98
Pietersburg (SAAF), S. Africa	23.9S x 29.5E	38	0.07	0.09	0.99	-0.03	0.98
Johannesburg, S. Africa	26.1S x 28.2E	41	0.04	0.07	1.06	-0.38	0.99
Canberra, Australlia	35.3S x 149.2E	35	0.04	0.06	0.99	0.00	1.00
		AVE =	0.06	0.19	1.00	-0.03	0.94
		STD =	0.15	0.16	0.14	0.86	0.15

VI.B.ii SSE vs Direct Measurements of Tilted Surface Insolation. Figure VI.1 show the time
series of the monthly mean solar insolation derived from measurements and the corresponding
values from SSE. Figure VI.1a gives the measured and SSE solar insolation on a horizontal
surface and Figure VI.b gives the measured and SSE values on a South facing surface tilted at
45°. The measured values were taken from the University of Oregon Solar Radiation
Monitoring Laboratory archive (http://solardat.uoregon.edu/index.html) for Chaney, WA.   For
comparison the RETScreen values have also been included.

*Figure VI.1Monthly time series of solar insolation measure on a horizontal (a) and tilted (b) surface at the University of
Oregon Solar Radiation Monitoring Laboratory Chaney, WA station, and corresponding insolation from RETScreen and
SSE. (Note that solar radiation is in KWh/day/m^2; multiplying KWh/day/m^2 by 41.67 yields W/m^2, and by 3.6 yields
MJ/day/m^2.)*

VII.B.iii SSE vs BSRN Based Tilted Surface Insolation. Solar insolation measurements at the
most of the ground sites in the Base Line Surface Network include the diffuse and direct normal
components as well as a direct measurement of the global, or total, insolation on a horizontal
surface. These measurements are typically made with at 1-, 2-, 3- or 5-minute intervals
throughout the day. The diffuse and direct normal measurements, coupled with the solar zenith
angle, provide the necessary components to estimate solar insolation on a tilted surface as
outlined below.

For any given BSRN site, consider a 3-D coordinate system with the origin at the BSRN site, X-
axis pointing eastward, Y-axis northward, and Z-axis upward. For any given instant
corresponding to a BSRN record, the unit vector pointing to the Sun is {sin(Z)cos[(π/2)-A]*i*,
sin(Z)sin[(π/2)-A]*j*, cos(Z)*k*}, and the unit vector along the normal of the titled surface is [0*i*, -
sin(T)*j*, cos(T)*k*] for Northern Hemisphere, and [0*i*, sin(T)*j*, cos(T)*k*] for Southern Hemisphere,
where Z is the solar zenith angle, A is the azimuth angle of the Sun, and T is the tilt angle of the
tilted surface. And the direct flux on the tilted surface is the direct normal flux times the dot
product of the aforementioned two unit vectors which is -sin(Z)cos(A)sin(T)+cos(Z)cos(T) for
Northern Hemisphere and sin(Z)cos(A)sin(T)+cos(Z)cos(T) for Southern Hemisphere. If the dot

product of the two unit vectors is less than zero, which means the Sun is behind the tilted surface, the direct flux on the tilted surface is set to zero. After this conversion, the 3-hourly, daily and monthly means of the direct component on the tilted surface can then be derived, and the diffuse component can be similarly derived. The sum of the direct and diffuse components is the total flux on the tilted surface.

Figure VI.2 is a scatter plot of the climatological monthly mean insolation on a tilted surface derived from the BSRN measurements of the diffuse and direct normal components versus the corresponding SSE tilted surface radiation values.

Figure VI.2 scatter plot of the climatological monthly mean insolation on a tilted surface derived from the BSRN measurements of the diffuse and direct normal components versus the corresponding SSE tilted surface radiation values. (Note that solar radiation is in KWh/day/m^2; multiplying KWh/day/m^2 by 41.67 yields W/m^2, and by 3.6 yields MJ/day/m^2.)
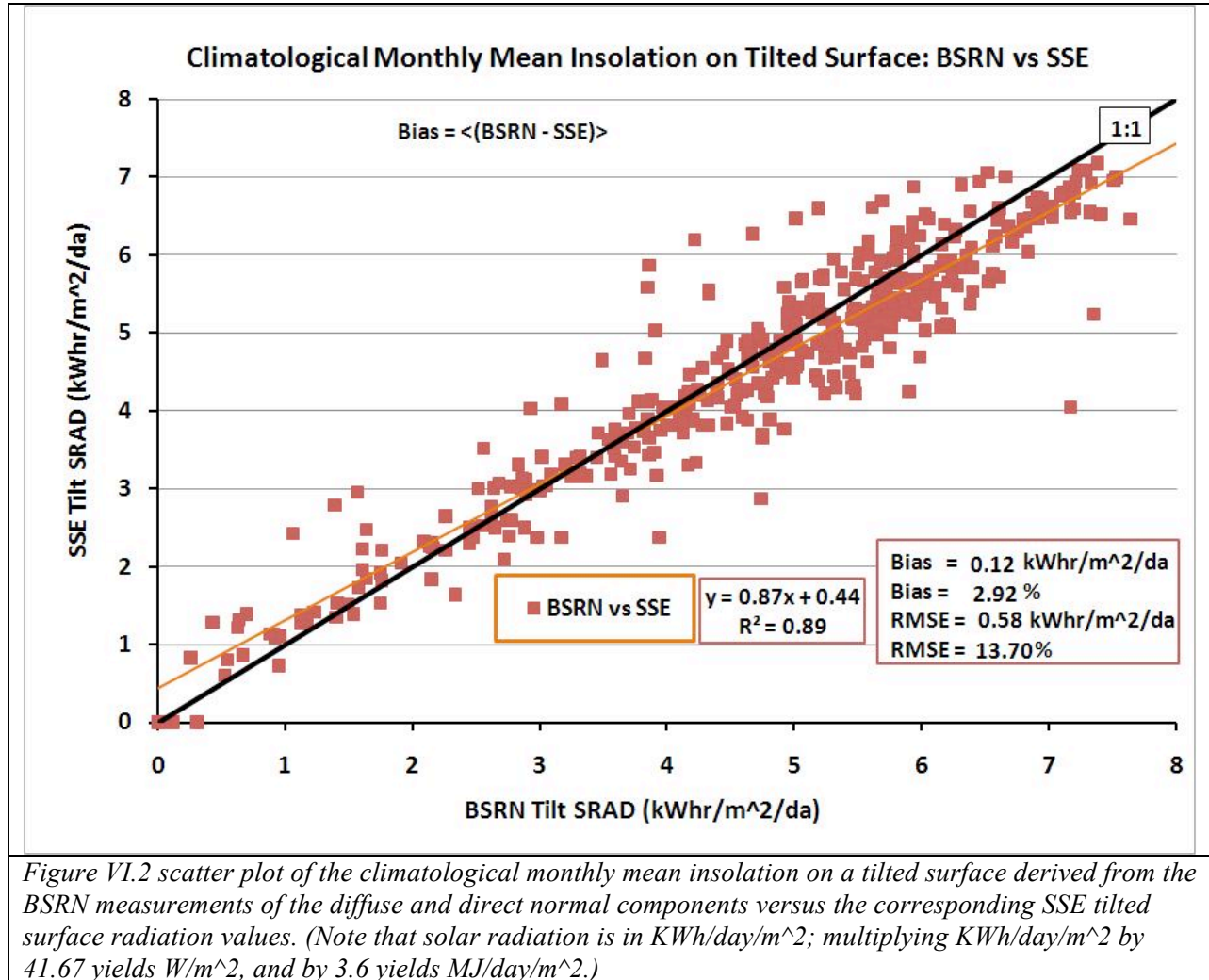
VII. Meteorological Parameters

The global distribution of meteorological parameters in the SSE archive are obtained from NASA's Global Model and Assimilation Office (GMAO), Goddard Earth Observing System

global assimilation model version 4 (GEOS-4) (http://gmao.gsfc.nasa.gov/systems/geos4/). Briefly, the meteorological parameters emerging from the GEOS-4 model are estimated via "An atmospheric analysis performed within a data assimilation context [that] seeks to combine in some "optimal" fashion the information from irregularly distributed atmospheric observations with a model state obtained from a forecast initialized from a previous analysis." (Bloom, et al., 2005). The model seeks to assimilate and optimize observational data and model estimates of atmospheric variables. Types of observations used in the GEOS-4 analysis include (1) land surface observations of surface pressure; (2) ocean surface observations of sea level pressure and winds; (3) sea level winds inferred from backscatter returns from space-borne radars; (4) conventional upper-air data from rawinsondes (e.g., height, temperature, wind and moisture); (5) additional sources of upper-air data include drop sondes, pilot balloons, and aircraft winds; and (6) remotely sensed information from satellites (e.g., height and moisture profiles, total precipitable water, and single level cloud motion vector winds obtained from geostationary satellite images). Emerging from the GEOS-4 analysis are 3-hourly global estimates of the vertical distribution of a range of atmospheric parameters.

The GEOS-4 data products are initially output on a 1^0 by 1.25^0 grid at 50 atmospheric levels, on 3-hourly time steps (e.g. 0, 3, 6, 9, 12, 15, 18, and 21 GMT). For use by the SRB retrieval (see section IV-B), the GEOS-4 products are bi-linearly interpolated to a 1^0 by 1^0 grid. Table III-2 lists the basic meteorological parameters that the SSE project obtains from GEOS-4.

(Return to Content)

***A. Assessment of the Daily Mean and Daily Maximum and Minimum GEOS-4 Temperatures*:**
In addition to the analysis reported by the NASA's Global Model and Assimilation Office (GMAO) (Bloom, et al.), the SSE project initiated a study focused on determining the accuracy of the GEOS-4 meteorological parameters in terms of the applications within the SSE project. In particular, the GEOS-4 temperatures (minimum, maximum and daily averaged air and dew point), relative humidity, and surface pressure have been explicitly compared to global data obtained from the National Climate Data Center (NCDC - http://www.ncdc.noaa.gov/oa/ncdc.html) Global Surface Summary of Day (GSOD) data, and to observations from other high quality networks such as the Surface Radiation (SURFRAD - http://www.srrb.noaa.gov/surfrad/index.html), Atmospheric Radiation Measurement (ARM - http://www.arm.gov/), as well as observations from automated weather data networks such as the High Plains Regional Climate Center (HPRCC - http://www.hprcc.unl.edu/index.php).

In this section we focus primarily on the analysis of the GEOS-4 daily maximum and minimum temperatures, and the daily mean temperature using observations reported in the NCDC GSOD files, with only summary comments regarding results from the other observational networks noted above. The GEOS-4 meteorological data in the SSE archive spans the same 22 year period as that of the solar parameters (i.e. July 1, 1983 - through June 30 2005) with the temperatures and humidity related parameters are based upon the GEOS-4 estimates at 10 m meters above the earth's surface.

In this section the analysis focuses on the daily Tmin, Tmax and Tave with a temporal coverage from January 1, 1983 – December 31, 2006. At each observational station in the NCDC GSOD files, the daily Tmin, Tmax and Tave were derived from the hourly observations filtered by an "85%" selection criteria applied to the observations reported for each station. Namely, only data from NCDC stations reporting 85% or greater of the possible 1-hourly observations per day and 85% or greater of the possible days per month were used to determine the daily Tmin, Tmax and Tave included in comparisons with the GEOS-4 derived data. Figure VII-A.1 illustrates the global distribution of the surface stations remaining in the NCDC data files for 1983 and 2004 after applying our 85% selection criteria. Note that the number of stations more that doubled from 1983 (e.g. 1104 stations) to 2004 (e.g. 2704 stations), and that majority of the stations are located in the northern hemisphere.

Figure VII-A.1: Top (a) and bottom (b) figures show distribution of NCDC stations meeting 85% selection criteria for 1987 and 2004, respectively.
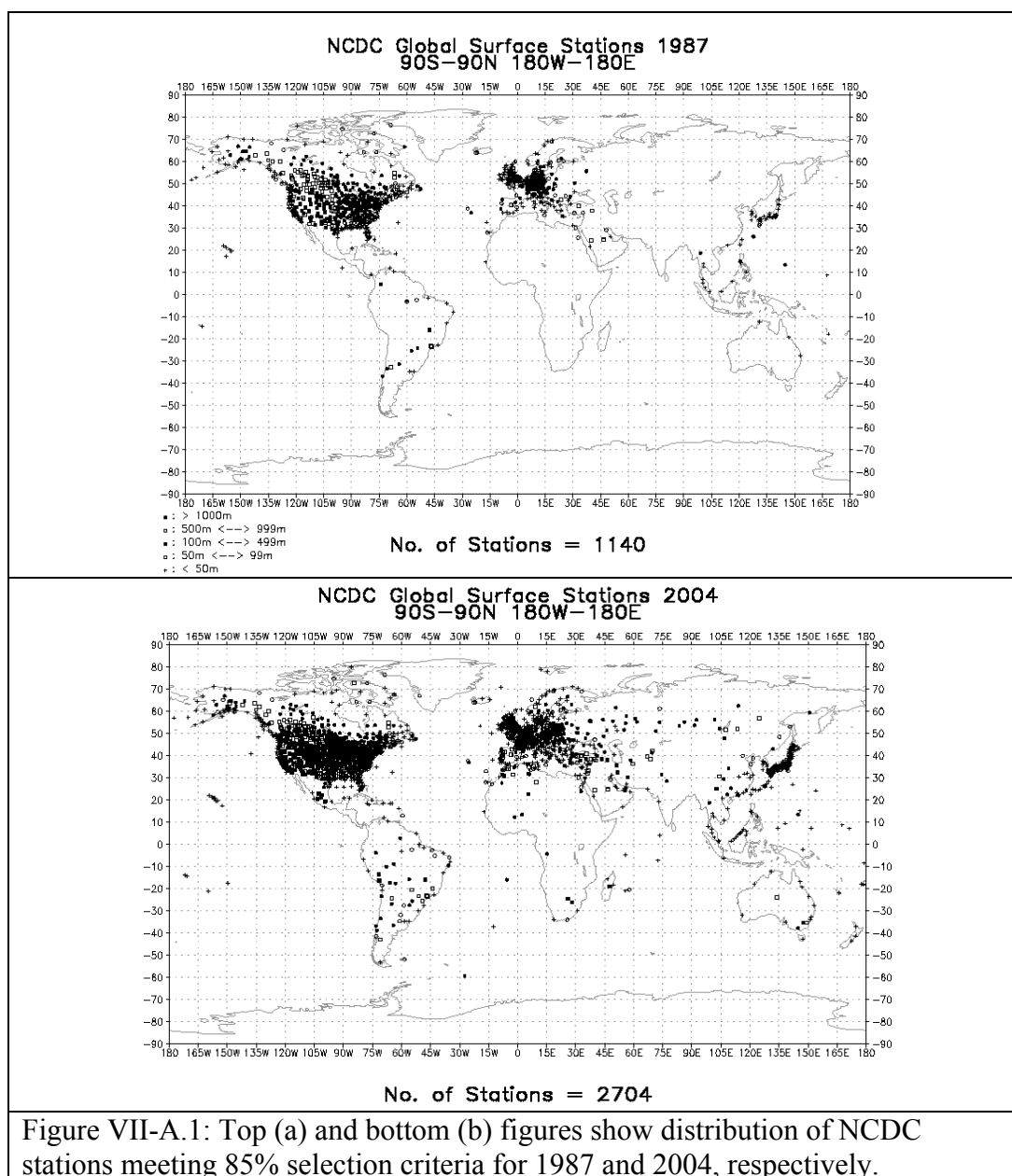
Unless specifically noted otherwise, all GEOS-4 air temperatures represent the average value on a 1° x 1° latitude, longitude grid cell at an elevation of 2 m above the earth's surface and NCDC values are ground observations at an elevation of 2 meters above the earth's surface. Figures VII-A.2a, -A.2b, and –A.2c, show, scatter plots of Tmin, Tmax and Tave derived from ground observations in the NCDC files versus GEOS-4 values for the years 1987 and 2004. These plots illustrate the agreement typically observed for all the years 1983 through 2006. In the upper left corner of each figure are the parameters for the linear least squares regression fit to theses data, along with the mean Bias and RMSE between the GEOS-4 and NCDC observations. The mean Bias Error (MBE) and RMSE are given as:

$$\text{MBE} = \sum_j \{ \sum_i \{ [(T_i^j)_{GEOS4} - (T_i^j)_{NCDC}] \} \} / N$$

$$\text{RMSE} = \{ \sum_j \{ \sum_i \{ [(T_i^j)_{GEOS4} - (T_i^j)_{NCDC}]^2 / N \} \} \}^{1/2},$$

where, $\sum_i$ is summation over all days meeting the 85% selection criteria, $\sum_j$ indicates the sum over all stations, $(T_i^j)_{NCDC}$ is the temperature on day i for station j, and $(T_i^j)_{GEOS4}$ is the GEOS-4 temperature corresponding to the overlapping GEOS-4 1-degree cell for day i and station j, and N is the number of matching pairs of NCDC and GEOS-4 values.

For the year 1987, 1139 stations passed our 85% selection criteria yielding 415,645 matching pairs on NCDC/GEOS-4 values; for 2004, 2697 stations passed yielding 987,451 matching pairs of NCDC/GEOS-4 temperature values. The color bar along the right side of the scatter plot provides a measure of the distribution of the NCDC/GEOS-4 temperature pairs. For example, in Figure III-A.2a, each data point shown in dark blue represents a 1-degree cell with 1 to 765 matching temperature pairs, and all of the 1-degree cells shown in dark blue contain 15.15% of the total number of ground site points. Likewise, the darkest orange color represent 1-degree cells for which there are from 6120 to 6885 matching temperature pairs, and taken as a group all of the 1-degree cells represented by orange contain 10.61% if the total number of matching
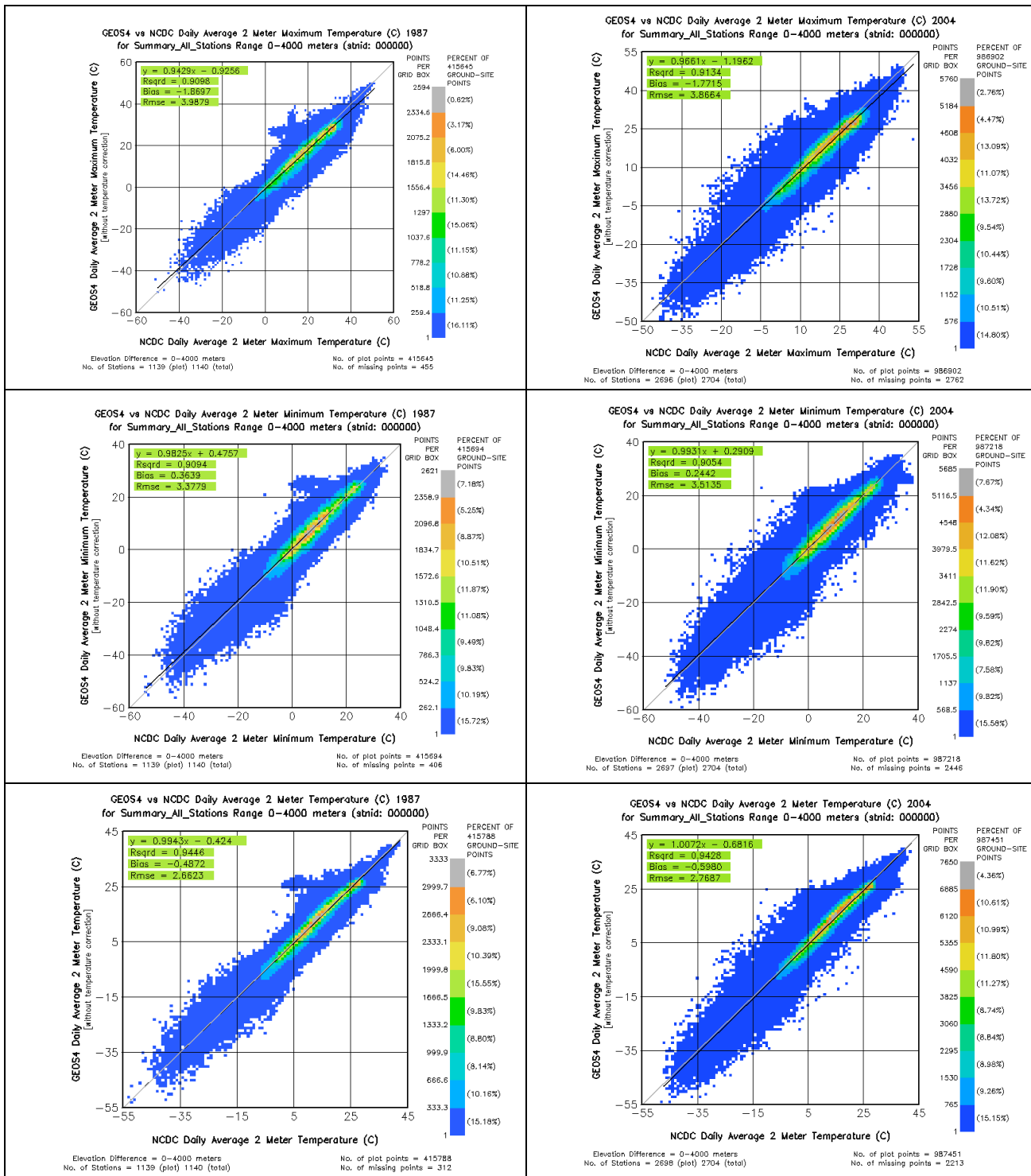
Figure VII-A.2. Top (a), middle (b) and bottom (c) figures show the scatter plot of ground site observations versus GEOS-4 values of Tmin, Tmax and Tave for the years 1987 and 2004. The color bar in each figure indicates the number and percentage of ground stations that are included within each color range. (WRS)

ground site points. Thus, for the data shown in Figure VII-A.2a, approximately 85% of matching temperature pairs (i.e. excluding the data represented by the dark blue color) is "tightly" grouped along the 1:1 correlation line.

In general, the scatter plots shown in Figure VII-A.2, and indeed for all the years from 1983 through 2006, exhibit good agreements between the GEOS-4 data and ground observations. Notice however that for both the 1987 and 2004 data, on a global basis, the GEOS-4 Tmax values are cooler than the ground values (e.g. bias = -1.9 C in 1987 and -1.8 C in 2004); the GEOS-4 Tmin values are warmer (e.g. bias = 0.4 $^{\circ}$ C in 1987 and 0.2 $^{\circ}$ C in 2004); and that GEOS-4 Tave values are cooler (e.g. bias = -0.5 $^{\circ}$ C in 1987, and -0.6 $^{\circ}$ C in 2004. Similar trends in the respective yearly averaged biases between GEOS-4 and NCDC observations were noted for each year from 1983 – 2006 (see Table VII-A.1 below). The ensemble average for the years 1983 – 2006 yields a GEOS-4 Tmax which is 1.82° C cooler than observed at NCDC ground Sites, a Tmin about 0.27° C warmer, and a Tave about 0.55° C cooler. Similar trends are also observed for measurements from other meteorological networks. For example, using the US National Weather Service Cooperative Observer Program (COOP) observations, White, et al (2008) found the mean values of GEOS-4 Tmax, Tmin, and Tave to be respectively 2.4° C cooler, Tmin 1.1° C warmer, and 0.7 $^{\circ}$ C cooler that the COOP values.

| Table VIII-A.1.Comparison of NCDC and GEOS-4 Temperatures with no corrections to GEOS-4 values. | | | | | | | | | | | | | | | | |
| | Tmax | | | | | Tmin | | | | | Tave | | | | |
Year	Slope	Intercept (C)	R^2	RMSE (C)	Bias (C)	Slope	Intercept (C)	R^2	RMSE (C)	Bias (C)	Slope	Intercept (C)	R^2	RMSE (C)	Bias (C)
2006	0.97	-1.28	0.92	3.88	-1.72	1.00	0.09	0.90	3.59	0.11	1.02	-0.79	0.94	2.82	-0.59
2005	0.97	-1.40	0.92	4.00	-1.92	0.99	0.20	0.91	3.57	0.16	1.01	-0.81	0.95	2.81	-0.67
2004	0.97	-1.20	0.91	3.86	-1.78	0.99	0.28	0.91	3.50	0.24	1.01	-0.69	0.94	2.76	-0.60
2003	0.95	-0.91	0.91	3.96	-1.74	0.99	0.46	0.91	3.49	0.38	1.00	-0.47	0.94	2.82	-0.53
2002	0.94	-0.88	0.91	4.06	-1.94	0.98	0.47	0.90	3.55	0.30	0.98	-0.48	0.94	2.85	-0.66
2001	0.97	-1.69	0.92	4.00	-2.20	1.00	0.10	0.90	3.62	0.11	1.01	-0.97	0.95	2.78	-0.81
2000	0.97	-1.17	0.91	3.84	-1.67	1.00	0.25	0.91	3.50	0.27	1.01	-0.65	0.94	2.77	-0.52
1999	0.97	-1.25	0.91	3.80	-1.78	0.99	0.47	0.91	3.37	0.39	1.00	-0.60	0.95	2.63	-0.54
1998	0.98	-1.29	0.92	3.67	-1.71	0.99	0.11	0.91	3.27	0.07	1.01	-0.81	0.94	2.62	-0.68
1997	0.97	-1.20	0.92	3.64	-1.66	0.99	-0.01	0.91	3.30	-0.05	1.00	-0.72	0.95	2.67	-0.68
1996	0.95	-0.71	0.91	3.67	-1.56	0.98	0.27	0.91	3.31	0.15	0.99	-0.46	0.94	2.66	-0.55
1995	0.97	-1.44	0.92	3.93	-1.91	1.00	0.32	0.92	3.44	0.29	1.01	-0.69	0.95	2.69	-0.60
1994	0.98	-1.58	0.92	4.08	-1.93	1.00	-0.01	0.91	3.55	-0.04	1.01	-0.82	0.95	2.85	-0.71
1993	0.96	-1.22	0.92	3.93	-1.80	0.99	0.22	0.92	3.40	0.16	1.00	-0.51	0.95	2.68	-0.52
1992	0.95	-0.92	0.91	3.90	-1.70	0.98	0.43	0.90	3.46	0.33	1.00	-0.43	0.94	2.67	-0.43
1991	0.95	-1.05	0.91	4.14	-1.89	0.99	0.35	0.91	3.45	0.27	1.00	-0.45	0.94	2.80	-0.49
1990	0.95	-1.12	0.90	4.18	-1.94	0.99	0.40	0.91	3.49	0.35	1.00	-0.44	0.94	2.79	-0.49
1989	0.96	-1.18	0.91	4.15	-1.91	0.99	0.48	0.92	3.50	0.42	0.99	-0.40	0.95	2.79	-0.46
1988	0.95	-1.11	0.91	4.03	-1.90	0.99	0.55	0.91	3.38	0.47	1.00	-0.38	0.95	2.63	-0.42
1987	0.94	-0.93	0.91	3.99	-1.87	0.98	0.48	0.91	3.38	0.36	0.99	-0.42	0.94	2.66	-0.49
1986	0.95	-1.02	0.91	4.05	-1.88	0.98	0.52	0.91	3.37	0.39	0.99	-0.35	0.94	2.70	-0.45
1985	0.96	-1.11	0.92	4.03	-1.84	0.99	0.38	0.92	3.58	0.32	0.99	-0.44	0.95	2.83	-0.49
1984	0.96	-1.07	0.91	4.00	-1.79	1.00	0.44	0.91	3.46	0.41	1.00	-0.45	0.94	2.79	-0.47
1983	0.96	-1.19	0.91	4.02	-1.78	0.99	0.41	0.91	3.44	0.34	1.00	-0.49	0.94	2.82	-0.52
Average	0.96	-1.16	0.91	3.95	-1.82	0.99	0.32	0.91	3.46	0.26	1.00	-0.57	0.94	2.75	-0.56
STDEV	0.01	0.22	0.01	0.15	0.13	0.01	0.17	0.01	0.10	0.14	0.01	0.17	0.00	0.08	0.10

Analysis of the differences between the GEOS-4 temperatures and ground site observations shows that one of the chief factors affecting the bias between the reanalysis temperatures and ground site observations is the elevation difference between the reanalysis grid cell elevation and the ground site elevation. Figure VII-A.3 illustrates the spatial features associated with a reanalysis cell and a local ground site.
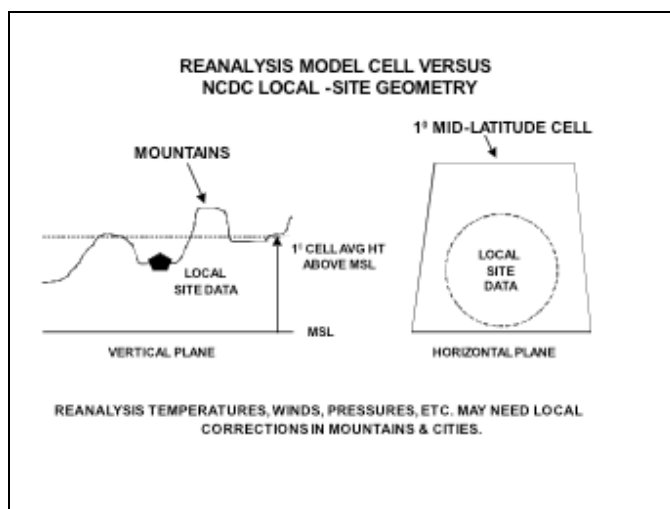
Figure VII-A.3*: Relative height and horizontal features associated with a 1-degree cell and a local ground site in the mountains.*

Note in particular that the elevation of a reanalysis cell is the average elevation of the earth's surface enclosed by the dimensions of the grid cell. In mountainous regions, in particular, the elevation of the grid cell can be substantially different from that of the underlying ground site.

In figure VII-A.4 the yearly averaged differences between ground site measurements and reanalysis modeled values (i.e. bias) are plotted against the difference in the elevation of the

(a)

(b)

Scatter Plot of Bias Between Uncorrected GEOS-4 and NCDC Daily 2-Meter Minimum Temperature and the Elevation Difference Between the GEOS-4 Cell and Ground Site for Years 1983-2006

y = -4.63x - 0.07
R² = 0.94
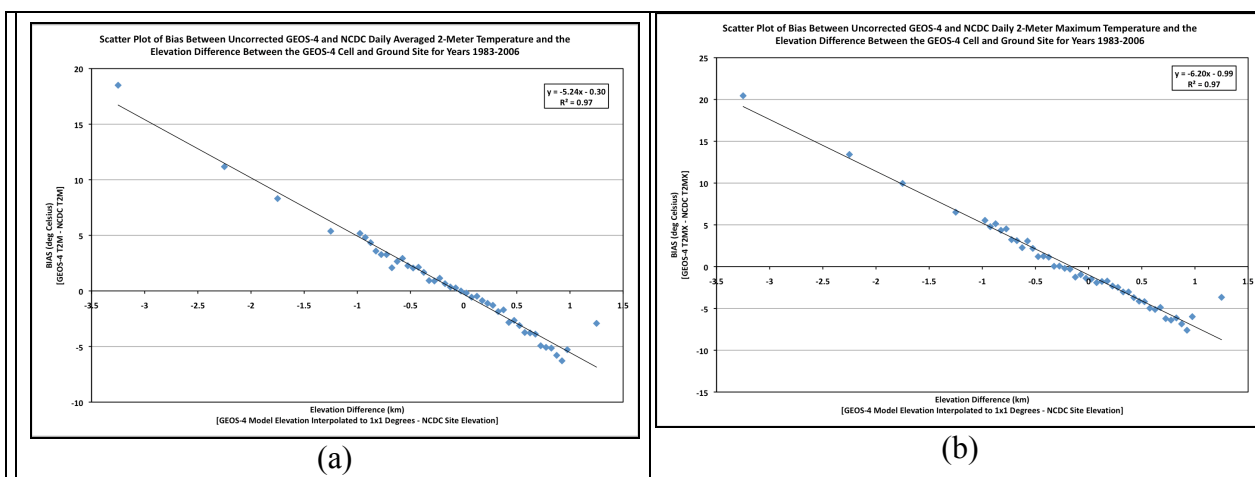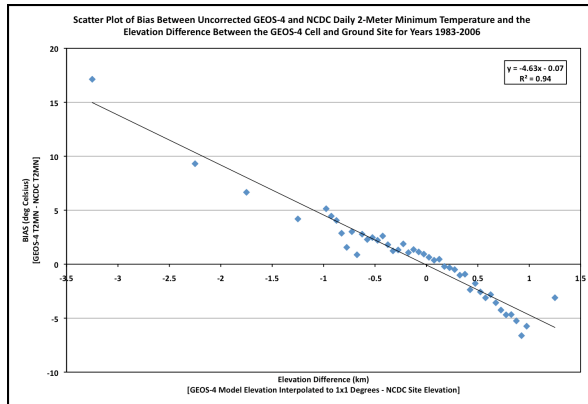
(c)

Figure VII-A.4. Scatter plots showing the dependence of the bias between the GEOS-4 Tave (a), Tmin (b), and Tmax (c) temperatures and values from the NCDC archive on the elevation difference between the GEOS-4 cell and the ground station elevation for the years 1983 -2006. The elevation difference between stations are grouped into elevation difference bins (e.g. 0 to 50m; >50m to 100m; >100m to 150m; etc.) and plotted against the mean bias for the respective elevation bin.

ground site and the reanalysis grid for the ensemble of years 1983 – 2006. The stations have been grouped into 50m elevation difference bins (e.g. 0 to 50m; >50m to 100m; >100m to 150m; etc.) and plotted against the mean yearly bias for the respective elevation bin. The solid line is the linear least squares fit to the scatter plot and the parameters for the fit are given in the upper right hand portion of each plot. Table VII-A.2 gives the parameters associated with linear regression fits to similar scatter plots for individual years and is included here to illustrate the year-to-year consistency in these parameters. The linear dependence of the bias between the GEOS-4 and NCDC temperature values on the elevation difference between the GEOS-4 cell and ground elevation is clearly evident in Figure VII-A.4 and Table VII-A.2. The mean of the slope, intercept, and R^2 for the individual years is given in the row labeled "Average". The bottom row of Table VII-A.2 lists the fit parameters of Figure VII-A.4.

Table VII-A.2. Linear regression parameters associated with scatter plots of yearly mean bias between NCDC and GEOS-4 daily tenperatures and the elevation difference between the NCDC ground station and the GEOS-4 1-degree grid cell. Each row gives the regression parameters by year. For comparison, the bottom row gives the regression parameters from Figure VII-A.4

Year	Tmax			Tmin			Tave		
	Slope (c/km)	Intercept (C)	R^2	Slope (c/km)	Intercept (C)	R^2	Slope (c/km)	Intercept (C)	R^2
1983	-5.56	-0.85	0.85	-3.9	0.37	0.87	-4.71	0.03	0.92
1984	-5.82	-0.71	0.87	-4.18	0.43	0.89	-4.98	0.1	0.93
1985	-4.96	-1.01	0.85	-4.11	0.3	0.84	-4.71	-0.05	0.94
1986	-5.64	-0.86	0.86	-4.11	0.31	0.84	-4.97	0.03	0.92
1987	-5.01	-1.17	0.82	-4.76	0.55	0.91	-4.84	-0.06	0.94
1988	-5.55	-0.91	0.83	-4.38	0.4	0.84	-4.95	0.04	0.9
1989	-5.37	-1.11	0.87	-3.82	0.15	0.81	-4.5	-0.23	0.9
1990	-6.7	-0.61	0.94	-4.85	0.3	0.9	-5.64	0.13	0.95
1991	-6.66	-0.41	0.93	-4.94	0.5	0.92	-5.73	0.32	0.96
1992	-6.29	-0.34	0.89	-5.09	0.75	0.91	-5.49	0.33	0.94
1993	-6.14	-0.35	0.89	-5.02	0.75	0.89	-5.5	0.48	0.93
1994	-6.38	-0.41	0.9	-5.42	0.67	0.9	-5.77	0.41	0.93
1995	-6.31	-0.78	0.9	-5.38	1	0.9	-5.71	0.32	0.93
1996	-6.14	0.04	0.88	-5.24	0.99	0.93	-5.59	0.6	0.94
1997	-6.55	-0.05	0.9	-5.18	0.64	0.92	-5.71	0.43	0.93
1998	-6.39	-0.28	0.91	-4.91	0.69	0.91	-5.5	0.34	0.94
1999	-6.68	-0.14	0.91	-4.95	0.92	0.93	-5.69	0.53	0.95
2000	-6.14	-0.24	0.93	-4.5	0.6	0.89	-5.23	0.34	0.94
2001	-5.72	-1.04	0.87	-4.27	0.2	0.82	-4.99	-0.17	0.92
2002	-6.38	-0.12	0.91	-4.5	0.71	0.89	-5.32	0.42	0.93
2003	-6.15	-0.04	0.93	-4.12	0.49	0.9	-5.03	0.37	0.95
2004	-6.32	-0.03	0.91	-4.48	0.57	0.9	-5.26	0.41	0.92
2005	-6.25	-0.38	0.93	-4.33	0.35	0.9	-5.18	0.18	0.94
2006	-6.09	-0.23	0.88	-4.44	0.27	0.88	-5.15	0.24	0.91
Average	-6.05	-0.50	0.89	-4.62	0.54	0.89	-5.26	0.23	0.93
STDEV	0.49	0.38	0.03	0.47	0.24	0.03	0.38	0.23	0.02
All Years Regression (Fig. VII-A.4)	-6.22	-0.43	0.9	-4.66	0.56	0.89	-5.34	0.26	0.93

The inverse dependence of the air temperature on elevation is well known with -6.5°C/km typically accepted as a global environmentally averaged lapse rate value (Barry and Chorely 1987). Moreover, numerous studies have been published (Blandford et al., 2008; Lookingbill et al., 2003; Harlow et al., 2004) that highlight the need to use seasonal and regionally dependent lapse rates for the daily Tmin and Tmax values to adjustment ground site observations to un-sampled sites at different elevations. In the remaining sections, we describe an approach to downscale the reanalysis temperatures to a specific site within the reanalysis grid box which minimizes the bias between the reanalysis model values and ground site observations.

A-i. Downscaling Methodology

In the previous section we demonstrated that the bias between ground site observations and GEOS-4 temperature estimates are linearly dependent on the elevation differences between reanalysis grid cell and the ground site elevation. In this section we develop the mathematical methodology for downscaling the reanalysis temperatures to localized site values. In subsequent sections the validity of the downscaling approach is demonstrated.

If we assume that the reanalysis modeled temperatures estimates can in fact be downscaled based upon a lapse rate correction, then we can express the downscaled temperatures at a local ground site as

Eq. VII-1. $\qquad (T^{grd})_{RA} = (T^{nat})_{RA} + \lambda*(H_{grd} - H_{RA}) + \beta$

Where $(T^{grd})_{RA}$ is the downscaled reanalysis temperature, $(T^{nat})_{RA}$ is the native reanalysis value averaged over the reanalysis grid cell, λ is the seasonal/regional lapse rate (C/km) appropriate for the given ground site, H_{grd} and H_{RA} are the elevation for ground site and reanalysis grid cell respectively, and β is included to account for possible biases between the reanalysis model estimates and ground observations. Assuming that eq. VII.1 provides an accurate estimate of the air temperature we have

Eq. VII-2. $\qquad (T^{grd}) = (T^{grd})_{RA},$

where (T^{grd}) is the air temperature at the desired ground site.

Equation Eq. VII-1 and Eq. VII-2 can be combined to yield

Eq. VII-3. $\qquad (T^{grd}) = (T^{nat})_{RA} + \lambda*(H_{grd} - H_{RA}) + \beta$

or

Eq. VII-4. $\qquad \Delta T = \lambda*\Delta H + \beta$

where ΔT is the difference between the air temperature at the desired ground site and the reanalysis cell temperature or Bias, and ΔH is the difference between the elevation of the ground site and the model cell. Equation Eq. VII-4 gives a linear relation between ΔT and ΔH with the slope given by λ, the lapse rate, and an intercept value given by β. A linear least squares fit to a scatter plot of ΔT vs ΔH (i.e. Figure VII-A.4) yields λ, the lapse rate, and β, the model bias. These parameters can then be used to downscale the reanalysis temperature values to any ground site within a region that the λ and β values are valid. Note that this methodology lends itself to generating λ and β values averaged over any arbitrary time period and/or investigating other environmental factors such as the influence of the vegetation type on the downscaling methodology.

Recall that the scatter plots shown in Figure VII-1.A.4 are constructed using the yearly mean bias between GEOS-4 and NCDC temperatures (i.e. ΔT) vs the difference in the elevation between the GEOS-4 grid cell and the ground site (i.e. ΔH). Consequently, from Eq. Eq. VII-4 the slope and intercept associated with the linear fit to the scatter plot give a set of globally averaged λ and β parameters for downscaling the reanalysis temperatures Tave, Tmin, and Tmax to any geographical site. Table VII-A.4 summarizes the values for λ (e.g. lapse rate) and β (e.g. offset) based upon the use of the NCDC GSOD meteorological data as the "calibration" source.

Table VII-A.4. Yearly and globally averaged lapse rate and offset values for adjusting GEOS-4 temperatures to local ground site values (based upon 1983 – 2006 NCDC and GEOS-4 global data).		
	Lapse Rate (^{o}C/km)	Off Set (^{o}C)
Tmax	-6.20	-0.99
Tmin	-4.63	-0.07
Tave	-5.24	-0.30

Figure VII-A.5 illustrates that bias between the ground observations and the GEOS-4 values after applying the lapse rate correction and offset values given in Table VII-A.4 is independent of the elevation difference between the ground site and the GEOS-4 1-degree cell and that the average bias is also near zero.

The values given in Table VII-A.4 are based upon the globally distributed ground sites in the NCDC GSOD database, and are based upon yearly mean ground and GEOS-4 data. The temperature parameters provided through the SSE online archive are either native values (i.e. un-adjusted) or downscaled values depending upon whether the users specifies the elevation of his/her location. When the elevation is provided, the downscaled temperatures are based upon the downscaling parameters (λ and β values) given in Table VII-A.4.

(a)

(b)

(c)
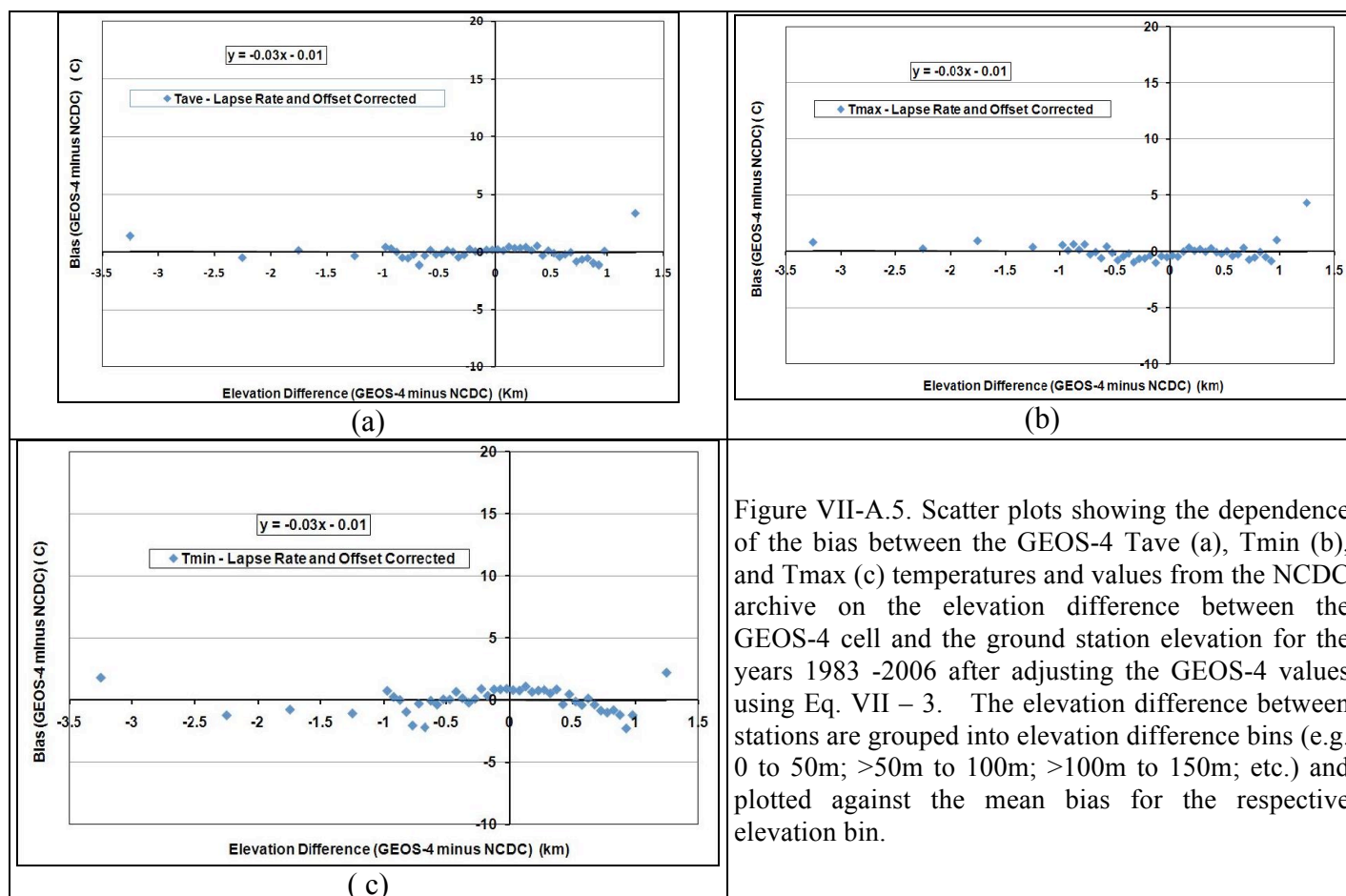
Figure VII-A.5. Scatter plots showing the dependence of the bias between the GEOS-4 Tave (a), Tmin (b), and Tmax (c) temperatures and values from the NCDC archive on the elevation difference between the GEOS-4 cell and the ground station elevation for the years 1983 -2006 after adjusting the GEOS-4 values using Eq. VII – 3.   The elevation difference between stations are grouped into elevation difference bins (e.g. 0 to 50m; >50m to 100m; >100m to 150m; etc.) and plotted against the mean bias for the respective elevation bin.

A.ii Global Downscaling: Table VII-A.5 gives the yearly mean global MBE and RMSE of the native (i.e. uncorrected) and downscaled GEOS-4 temperature values relative to NCDC values for the year 2007. The 2007 GEOS-4 values were downscaled via Eq. VII-3 using the lapse rate and offset parameters given in Table VIII-A.4. Since the λ and β parameters for downscaling were developed using NCDC data over the years 1983 – 2006, the use of data from 2007 serves as an independent data set for this test.

Table VII-A.5. Yearly Mean Bias Error (MBE) and Root Mean Square Error (RMSE) for 2007 native and downscaled GEOS-4 temperatures relative to NCDC temperatures. The downscaled GEOS-4 values are based upon the downscaling parameters given in Table VII-A.4.

		Native GEOS-4	Downscaled GEOS-4
Tmax	**MBE**	-1.58	-0.10
	RMSE	3.79	3.17
Tmin	**MBE**	0.27	0.71
	RMSE	3.57	3.42
Tave	**MBE**	-0.50	0.22
	RMSE	2.82	2.47

The lapse rates and offset values given in Table VII-A.4 are yearly averaged values based upon a globally distributed ground sites in the NCDC data base. The temperature parameters provided through the SSE are either native values (i.e. un-adjusted) or downscaled values depending upon whether the user specifies the elevation of his/her location. When the elevation is provided, the downscaled temperatures are based upon the downscaling parameters (λ and β values) given in Table VII-A.4.

Results from a number of studies have indicated that tropospheric lapse rates can be seasonally and regionally dependent. Accordingly, Table VII-A.6 gives the globally and monthly averaged lapse rate and offset downscaling parameters for GEOS-4 temperatures. These parameters were developed from eq. Eq. VII-4 using the globally distributed NCDC temperature data over the years 1983 – 2006.

Table VII-A.6. Globally and monthly mean lapse rates and offset values for adjusting GEOS-4 temperatures to local ground site values. Based upon 1983 – 2006 NCDC and GEOS-4 global data.													
	JAN	FEB	MAR	APR	MAY	JUN	JUL	AUG	SEP	OCT	NOV	DEC	YR
Tmx λ	-5.12	-5.97	-6.73	-7.2	-7.14	-6.78	-6.52	-6.44	-6.31	-5.91	-5.44	-4.85	-6.22
Tmx β	-1.61	-1.57	-1.4	-1.01	-0.56	-0.29	-0.24	-0.46	-0.67	-1.08	-1.44	-1.55	-0.99
Tmn λ	-4.34	-4.89	-5.17	-5.16	-4.93	-4.67	-4.46	-4.33	-4.28	-4.31	-4.6	-4.44	-4.63
Tmn β	-0.96	-0.95	-0.69	-0.14	0.22	0.34	0.43	0.5	0.58	0.42	-0.06	-0.61	-0.07
Tm λ	-4.49	-5.19	-5.73	-6.06	-5.91	-5.59	-5.35	-5.27	-5.14	-4.9	-4.8	-4.45	-5.24
Tm β	-1.16	-1.09	-0.9	-0.34	0.17	0.42	0.51	0.35	0.13	-0.18	-0.61	-0.97	-0.3

Tables VII-A.7 and VII-A.8 give respectively the globally averaged monthly MBE and RMSE associated with the 2007 GEOS-4 uncorrected and downscaled temperatures relative to NCDC ground site values.

Table VII-A.7. Globally averaged monthly MBE and RMSE associated with uncorrected 2007 GEOS-4 temperatures relative to 2007 NCDC GSOD temperatures												
	JAN	**FEB**	**MAR**	**APR**	**MAY**	**JUN**	**JUL**	**AUG**	**SEP**	**OCT**	**NOV**	**DEC**	**YR**
Tmax MBE	-2.00	-2.11	-2.00	-1.64	-1.13	-1.15	-0.84	-1.27	-1.49	-1.85	-1.73	-1.90	-1.89
Tmax RMSE	4.04	4.00	4.01	3.75	3.73	3.64	3.57	3.64	3.66	3.72	3.71	4.02	3.79
Tmin MBE	-0.24	-0.49	-0.23	0.19	0.56	0.49	0.66	0.61	0.81	0.76	0.50	-0.41	0.27
Tmin RMSE	4.13	4.02	3.70	3.32	3.25	3.09	3.10	3.13	3.30	3.50	3.84	4.26	3.55
Tave MBE	-1.0	-1.15	-0.88	-0.54	-0.03	-0.06	-0.13	-0.18	-0.15	-0.43	-0.59	-1.08	-0.50
Tave RMSE	3.20	3.18	2.92	2.62	2.66	2.54	2.55	2.50	2.51	2.56	2.91	3.41	2.80

Table VII-A.8. Globally and monthly averaged MBE and RMSE associated with downscaled 2007 temperatures relative to 2007 NCDC GSOD temperatures. The GEOS-4 temperatures were downscaled using the global monthly averaged λ and β values given in Table VII-A.6.												
	JAN	**FEB**	**MAR**	**APR**	**MAY**	**JUN**	**JUL**	**AUG**	**SEP**	**OCT**	**NOV**	**DEC**	**YR**
Tmax MBE	0.04	-0.07	-0.04	-0.06	0.00	-0.32	-0.08	-0.30	-0.32	-0.29	0.14	0.04	-0.10
Tmax RMSE	3.35	3.11	3.17	2.97	3.18	3.16	3.18	3.13	3.02	2.98	3.06	3.40	3.14
Tmin MBE	1.06	0.85	0.87	0.74	0.74	0.52	0.59	0.45	0.57	0.69	0.92	0.56	0.71
Tmin RMSE	4.11	3.87	3.54	3.13	2.99	2.83	2.86	2.87	3.01	3.26	3.71	4.12	3.36
Tave MBE	0.52	0.33	0.48	0.28	0.27	-0.04	0.04	-0.11	0.13	0.14	0.41	0.25	0.22
Tave RMSE	2.94	2.69	2.44	2.11	2.22	2.18	2.24	2.16	2.12	2.20	2.61	3.06	2.41

A.ii. Regional Downscaling: As noted above, Eq. VII-4 can be used to develop regional specific λ and β values that, for some applications, may be more appropriate than the globally and yearly or globally and monthly averaged values of Table VII-A.4 or Table VII-A.6 respectively.   To illustrate the use of regional versus global based downscaling, λ and β values, the regional monthly averaged MBEs and RMSEs associated with comparing GEOS-4 temperatures to NCDC ground site values in the US Pacific Northwest region (40 - 50N, 125 – 110W) are given in Table VII-A.9a for uncorrected GEOS-4 temperatures; in Table VII-A.9b for downscaled

GEOS-4 temperatures using the global and monthly averaged λ and β values given in Table VII-A.6; and in Table VII-A.9.c for downscaled GEOS-4 temperatures using the regional monthly downscaling parameters derived for the Northwest Pacific region (given in Table VII-A.10).

Table VII-A.9a. MBE and RMSE associated with uncorrected 2007 GEOS-4 temperatures relative to 2007 NCDC GSOD temperatures in the US Pacific Northwest region (40 - 50N, 125 – 110W)

	JAN	FEB	MAR	APR	MAY	JUN	JUL	AUG	SEP	OCT	NOV	DEC	YR
Tmax MBE	-3.05	-3.41	-4.47	-3.96	-3.10	-3.47	-2.74	-3.23	-3.58	-3.77	-3.25	-3.18	-3.43
Tmax RMSE	5.06	5.11	5.78	5.34	5.06	5.18	4.85	5.28	5.63	5.36	4.99	4.76	5.20
Tmin MBE	-2.59	-2.90	-2.85	-2.30	-1.51	-1.50	-0.34	-0.12	-0.39	-1.19	-1.40	-2.94	-1.67
Tmin RMSE	5.58	5.32	5.03	4.45	4.18	4.36	4.25	4.22	4.33	3.95	4.71	5.53	4.66
Tave MBE	-2.40	-2.56	-3.12	-2.59	-1.52	-1.65	-0.83	-1.15	-1.54	-1.99	-2.11	-2.79	-2.02
Tave RMSE	4.36	4.12	4.33	3.92	3.33	3.38	3.16	3.21	3.41	3.48	3.92	4.52	3.76

Table VII-A.9b. MBE and RMSE associated with downscaled 2007 temperatures relative to 2007 NCDC GSOD temperatures in the US Pacific Northwest region (40 - 50N, 125 – 110W). The GEOS-4 temperatures were downscaled using the global and monthly averaged λ and β values given in Table VII-A.6.

	JAN	FEB	MAR	APR	MAY	JUN	JUL	AUG	SEP	OCT	NOV	DEC	YR
Tmax MBE	0.42	0.33	-0.63	-0.33	0.05	-0.72	-0.13	-0.43	-0.63	-0.54	0.16	0.13	-0.19
Tmax RMSE	4.02	3.60	3.48	3.08	3.71	3.62	3.86	4.05	4.24	3.71	3.67	3.28	3.69
Tmin MBE	-0.06	-0.17	-0.29	-0.29	0.05	-0.15	0.85	0.95	0.58	-0.04	0.33	-0.72	0.09
Tmin RMSE	4.61	4.02	3.67	3.28	3.41	3.55	3.85	3.85	3.95	3.41	4.10	4.40	3.84
Tave MBE	0.39	0.42	-0.15	-0.05	0.45	-0.05	0.60	0.41	0.20	-0.03	0.24	-0.20	0.18
Tave RMSE	3.42	2.82	2.44	2.13	2.37	2.34	2.64	2.50	2.50	2.45	2.93	3.25	2.65

Table VII-A.9c MBE and RMSE associated with downscaled 2007 temperatures relative to 2007 NCDC GSOD temperatures in the US Pacific Northwest region (40 - 50N, 125 – 110W). The GEOS-4 temperatures were downscaled using the regional and monthly averaged λ and β values given in Table VII-A.10.

	JAN	FEB	MAR	APR	MAY	JUN	JUL	AUG	SEP	OCT	NOV	DEC	YR
Tmax MBE	0.28	0.54	-0.11	0.45	0.70	0.05	0.58	0.54	0.45	0.50	0.51	-0.39	0.34
Tmax RMSE	4.00	3.63	3.45	3.11	3.77	3.55	3.90	4.05	4.21	3.70	3.71	3.30	3.70
Tmin MBE	0.32	0.14	-0.32	-0.41	0.01	-0.23	0.20	0.18	0.00	-0.31	0.30	-0.32	-0.04
Tmin RMSE	4.58	3.96	3.62	3.25	3.38	3.49	3.70	3.71	3.88	3.41	4.05	4.31	3.78
Tave MBE	0.35	0.46	-0.07	0.10	0.46	-0.08	0.33	0.28	0.28	0.15	0.22	-0.36	0.18
Tave RMSE	3.41	2.81	2.42	2.09	2.36	2.32	2.58	2.47	2.49	2.45	2.91	3.25	2.63

Table VII-A.10. Regional and monthly mean lapse rate and offset values for adjusting GEOS-4 temperatures to local ground sites in the US Pacific Northwest region. Based upon 1983 – 2006 NCDC and GEOS-4 temperatures in the US Pacific Northwest region.

	JAN	FEB	MAR	APR	MAY	JUN	JUL	AUG	SEP	OCT	NOV	DEC	YR
Tmax λ	-5.13	-6.22	-7.54	-7.88	-7.09	-6.61	-6.29	-5.87	-6.09	-5.83	-5.56	-4.69	-6.23
Tmax β	-1.47	-1.69	-1.63	-1.55	-1.23	-1.12	-1.03	-1.64	-1.82	-2.15	-1.74	-1.09	-1.51
Tmin λ	-5.55	-6.46	-6.68	-6.06	-5.53	-5.64	-5.25	-4.77	-4.7	-4.64	-5.54	-5.37	-5.51
Tmin β	-0.9	-0.69	-0.12	0.31	0.48	0.78	1.36	1.43	1.31	0.81	0.31	-0.68	0.37
Tave λ	-5.35	-6.38	-7.11	-7.26	-6.55	-6.27	-5.87	-5.54	-5.58	-5.39	-5.55	-5.02	-5.98
Tave β	-0.81	-0.7	-0.48	-0.06	0.4	0.7	0.97	0.58	0.2	-0.19	-0.32	-0.61	-0.02

The monthly time series of MBE and RMSE associated with the US Pacific Northwest are plotted in Figures VII.A.6 for the uncorrected GEOS-4 and GEOS-4 downscaled using (1) yearly and global mean lapse rate and offset values, (2) monthly mean global lapse rate and offset values, (3) yearly mean regional lapse rate and offset values, and (4) monthly mean regional lapse rate and offset values. For each set of downscaling parameters (i.e. lapse rate and offset) there is a substantial reduction in the MBE and RMSE; however, there is little difference in the RMSE values relative to the temporal averaging period (i.e. yearly vs. monthly average) or geographical region (global vs. regional) used to generate the downscaling parameters. The MBE is however somewhat more dependent on the set of downscaling parameters, with the monthly mean regional values yielding the lowest MBE error particularly in the MBE for Tmin.

The regional downscaling discussed here is not currently available through SSE, and is discussed here only to give an interested User guidance in its application.
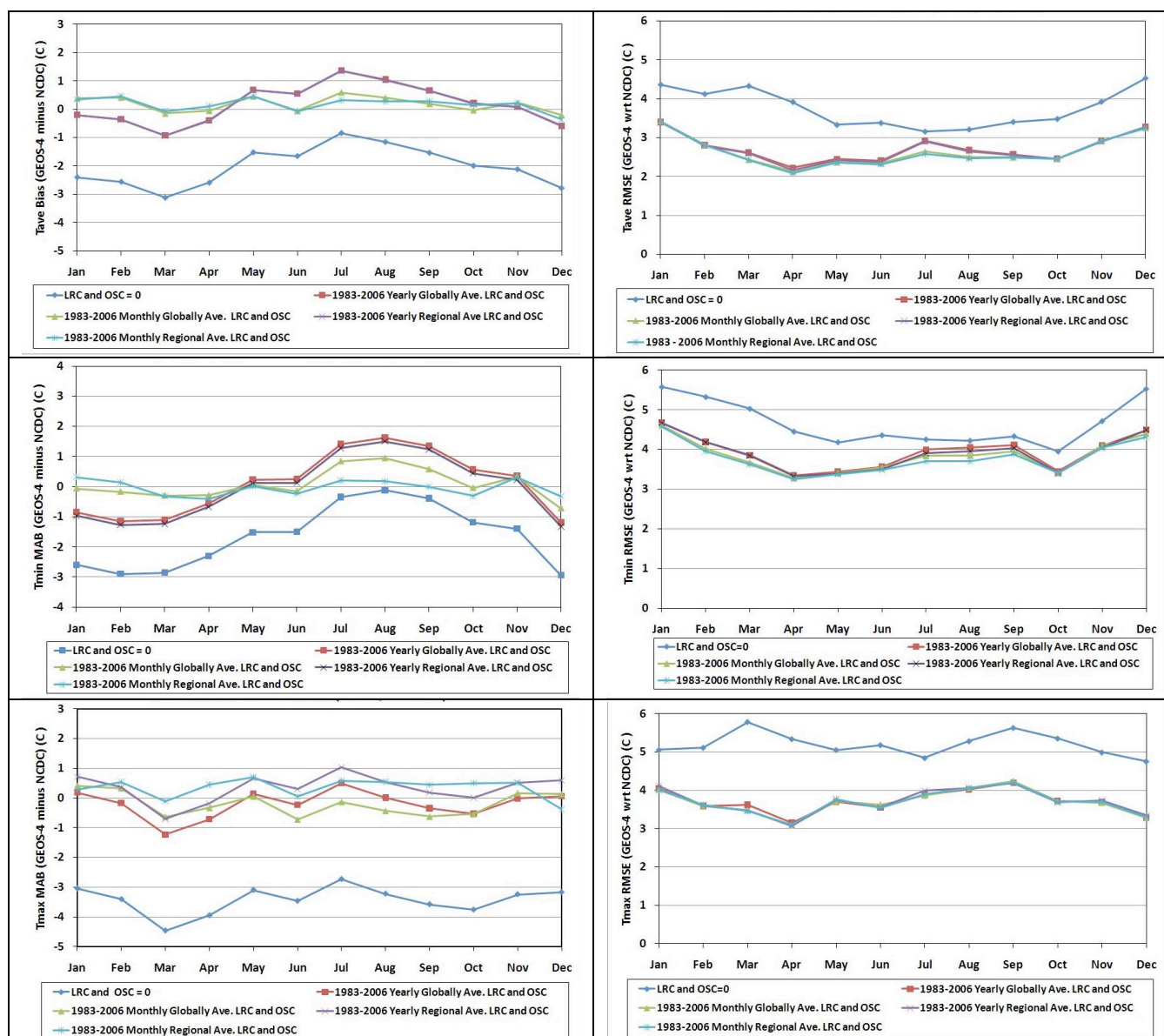
Figure VII.A.6. Monthly time series of the MBE (left column) and RMSE (right column) between 2007 un-scaled and downscaled GEOS-4 and NCDC ground sites observations in the Pacific Northwest region (40 - 50N, 125 – 110W). The MBE and RMSE monthly time series values are plotted for the (1) uncorrected GEOS-4 (i.e. LRC and OSC = 0) and GEOS-4 corrected using (2) yearly and global mean lapse rate and offset values, (3) monthly mean global lapse rate and offset values, (4) yearly mean regional lapse rate and offset values, and (5) monthly mean regional lapse rate and offset values. The downscaling parameters are based upon GEOS-4 and NCDC station temperatures over the years 1983 – 2006.

VII-B. *Heating/Cooling Degree Days:*

An important application of the historical temperature data is in the evaluation of heating and cooling degree days. Table VII-A.1 and VII-A.2 provide information relative to the use of GEOS-4 temperature corrected and uncorrected versus NCDC values to evaluate the yearly heating degree days (HDD) and cooling degree days (CDD). The HDD and CDD are based upon the daily Tmin and Tmax with a base temperature, Tbase = 18^0C. The HDD and CDD were calculated using the following equations:

Heating Degree Days: For the days of a given time period (e.g. year, month, etc.) sum the quantity
[Tbase - (Tmin + Tmax) / 2] when (Tmin + Tmax) / 2 < Tbase

Cooling Degree Days: For the days of a given time period (e.g. year, month, etc.) sum the quantity
[((Tmin + Tmax) / 2) - Tbase] when (Tmin + Tmax) / 2 > Tbase.

Values given in Table VII-A.ii.1 used the uncorrected GEOS-4 temperatures while values in Table VII-A.ii.2 used GEOS-4 Tmax and Tmin values corrected as per Eq. VII-A.1. The bottom row in each table provides the overall estimates of the agreement between the two data sets for the years 1983 – 2006. The average over the years is the straight average of the values for the individual years listed in the tables. It is important to note that the use of the GEOS-4 temperature adjusted for elevation differences between the GEOS-4 grid cell and ground site elevation (e.g. lapse rate correction) and the appropriate offsets result in a significant improvement in the agreements between the GEOS-4 and NCDC based HDD and CDD, particularly in the bias values.

Table VII-B.ii.1

	Table VIII-A.ii.1. Comparison of the yearly heating and cooling degree days based upon NCDC vs GEOS-4 temperature data. No corrections to GEOS-4 values.												
	Heating Degree Days (Tmax, Tmin)							Cooling Degree Days (Tmax, Tmin)					
Year	Bias (HDD)	Bias %	RMSE (HDD)	RMSE %	Slope	Intercept (HDD)	R^2	Bias (CDD)	Bias %	RMSE (CDD)	RMSE %	Slope	Intercept (CDD)	R^2
1983	16.30	6.44	68.59	27.11	1.03	9.85	0.95	-4.78	-8.93	28.53	53.34	0.86	2.68	0.92
1984	16.37	6.34	64.45	24.97	1.03	8.46	0.95	-4.25	-8.35	27.01	53.07	0.86	2.86	0.92
1985	16.13	6.01	64.31	23.97	1.03	9.19	0.96	-5.96	-11.21	27.82	52.33	0.85	1.80	0.92
1986	14.07	5.55	85.41	33.72	0.98	18.25	0.91	-6.60	-12.50	27.73	52.56	0.84	1.91	0.93
1987	14.92	5.91	69.30	27.42	1.02	10.71	0.94	-6.21	-12.01	27.17	52.52	0.85	1.76	0.93
1988	15.20	6.20	65.39	26.68	1.03	6.79	0.95	-5.53	-10.10	27.39	50.05	0.86	2.22	0.93
1989	14.71	5.85	66.75	26.54	1.03	7.55	0.95	-6.29	-11.91	29.02	54.96	0.84	2.35	0.91
1990	16.84	7.09	66.45	27.97	1.04	7.67	0.95	-6.63	-11.92	28.70	51.60	0.83	2.66	0.93
1991	14.69	6.03	78.74	32.33	1.01	11.89	0.92	-6.93	-11.60	30.28	50.71	0.84	2.59	0.92
1992	12.94	5.19	79.58	31.91	1.00	12.11	0.92	-4.94	-10.62	25.52	54.79	0.86	1.80	0.92
1993	17.79	6.94	71.34	27.83	1.03	10.14	0.94	-5.32	-9.97	26.29	49.30	0.88	1.10	0.93
1994	22.88	9.24	72.22	29.17	1.05	11.59	0.95	-6.12	-10.75	27.96	49.09	0.87	1.36	0.93
1995	17.54	7.10	70.60	28.60	1.03	9.83	0.95	-5.38	-9.13	28.04	47.55	0.87	2.28	0.93
1996	10.15	4.64	99.68	45.60	0.93	25.32	0.84	-6.66	-10.70	30.31	48.68	0.86	2.09	0.92
1997	19.61	8.56	62.21	27.16	1.05	7.08	0.95	-6.39	-11.33	28.24	50.06	0.85	2.02	0.92
1998	24.65	11.56	68.35	32.06	1.09	5.74	0.94	-5.19	-8.91	27.48	47.17	0.87	2.30	0.93
1999	18.58	8.53	61.38	28.18	1.06	6.22	0.95	-3.92	-6.53	28.87	48.11	0.88	3.01	0.92
2000	17.61	7.32	66.54	27.67	1.05	6.15	0.95	-3.23	-6.06	27.74	52.00	0.88	3.06	0.92
2001	24.33	9.94	64.77	26.46	1.06	8.60	0.96	-7.08	-12.74	30.00	53.97	0.84	1.75	0.92
2002	16.62	6.92	67.75	28.22	1.03	9.73	0.94	-7.95	-13.80	29.96	52.00	0.83	1.58	0.92
2003	14.75	6.24	66.15	27.96	1.04	6.33	0.94	-5.84	-9.97	30.91	52.77	0.85	3.23	0.91
2004	16.52	6.87	90.29	37.56	1.00	17.33	0.90	-6.14	-11.66	27.97	53.10	0.84	2.19	0.92
2005	20.40	8.32	66.41	27.07	1.05	7.56	0.95	-5.80	-9.96	29.13	49.99	0.86	2.39	0.93
2006	16.56	6.76	126.66	51.69	0.91	39.49	0.81	-4.88	-8.89	29.25	53.28	0.87	2.44	0.92
Average of Individual Years	17.09	7.07	73.47	30.33	1.02	11.40	0.93	-5.75	-10.40	28.39	51.37	0.86	2.23	0.92

Table VII-B.ii.2

Table VIII-A.ii.2. Comparison of the yearly heating and cooling degree days based upon NCDC vs GEOS-4 temperature data.
GEOS-4 values have been lapse rate and offset corrected with values listed in Table VIII-A.4.

Year	Heating Degree Days (Tmax, Tmin)							Cooling Degree Days (Tmax, Tmin)						
	Bias (HDD)	Bias %	RMSE (HDD)	RMSE %	Slope	Intercept (HDD)	R^2	Bias (CDD)	Bias %	RMSE (CDD)	RMSE %	Slope	Intercept (CDD)	R^2
1983	0.48	0.19	57.56	22.75	1.01	-1.06	0.96	2.29	4.28	28.59	53.45	0.94	5.27	0.91
1984	0.06	0.02	52.69	20.41	1.01	-1.96	0.96	2.27	4.46	27.52	54.05	0.94	5.21	0.91
1985	-0.68	-0.25	54.86	20.45	1.00	-1.97	0.96	0.94	1.77	26.66	50.18	0.94	4.35	0.92
1986	-2.55	-1.01	78.34	30.93	0.96	6.42	0.92	0.38	0.72	25.87	49.01	0.92	4.61	0.93
1987	-0.79	-0.31	60.04	23.76	1.00	-0.16	0.95	0.42	0.81	25.74	49.74	0.93	4.11	0.93
1988	-0.35	-0.14	55.38	22.59	1.01	-3.68	0.96	1.14	2.08	26.62	48.64	0.94	4.62	0.93
1989	-0.58	-0.23	57.80	22.98	1.01	-3.33	0.96	0.37	0.70	27.79	52.63	0.91	4.93	0.91
1990	2.04	0.86	53.42	22.49	1.02	-2.71	0.96	0.16	0.29	26.45	47.55	0.91	5.09	0.93
1991	0.00	0.00	67.86	27.86	0.99	1.30	0.94	0.74	1.24	28.36	47.49	0.93	4.84	0.92
1992	-2.55	-1.02	69.80	27.99	0.99	0.69	0.93	1.83	3.93	23.87	51.24	0.95	4.13	0.93
1993	0.92	0.36	61.86	24.13	1.01	-1.93	0.95	1.84	3.46	25.96	48.68	0.96	4.07	0.93
1994	4.72	1.91	59.03	23.84	1.03	-1.85	0.96	1.97	3.46	28.10	49.32	0.96	4.41	0.92
1995	0.92	0.37	59.47	24.09	1.01	-2.25	0.96	2.27	3.85	27.28	46.27	0.95	5.31	0.93
1996	-5.88	-2.69	93.53	42.78	0.91	13.74	0.85	2.73	4.38	30.52	49.01	0.95	6.07	0.91
1997	2.86	1.25	47.93	20.92	1.03	-4.71	0.97	1.97	3.48	26.52	47.00	0.94	5.17	0.92
1998	7.41	3.48	53.79	25.23	1.06	-5.63	0.96	3.34	5.74	27.21	46.70	0.96	5.56	0.93
1999	2.32	1.06	47.22	21.68	1.03	-4.64	0.97	4.49	7.48	29.46	49.07	0.97	6.49	0.92
2000	0.45	0.19	51.64	21.48	1.03	-6.58	0.96	4.51	8.45	28.40	53.22	0.97	6.33	0.92
2001	6.89	2.82	49.99	20.42	1.04	-3.02	0.97	0.51	0.91	29.40	52.89	0.92	4.70	0.91
2002	0.25	0.11	55.07	22.94	1.01	-2.59	0.95	-0.24	-0.42	28.45	49.35	0.92	4.65	0.92
2003	-0.66	-0.28	53.93	22.80	1.02	-5.05	0.96	2.55	4.35	29.83	50.90	0.94	6.34	0.91
2004	-0.27	-0.11	81.18	33.77	0.98	4.36	0.91	1.82	3.45	26.77	50.80	0.93	5.33	0.92
2005	3.43	1.40	53.04	21.62	1.03	-4.88	0.96	1.85	3.17	28.47	48.84	0.94	5.40	0.92
2006	0.25	0.10	120.46	49.15	0.89	27.04	0.82	2.63	4.79	28.94	52.70	0.95	5.37	0.91
Average of Individual Years	0.78	0.34	62.33	25.71	1.00	-0.19	0.94	1.78	3.20	27.61	49.95	0.94	5.10	0.92

C. Surface Pressure:

Recognizing that improvement in the GEOS-4 temperatures can be achieved through adjustments associated with differences in the average elevation of the GEOS-4 1-degree cell and that of the ground site of interest suggest that other altitude dependent parameters, such as pressure, might also benefit in similar altitude related adjustments. Figures VII-B.1(a-c) illustrate significant improvements in the GEOS-4 surface pressure values (p) by using the hypsometric equation (VII-B.1), relating the thickness (h) between two isobaric surfaces to the mean temperature (T) of the layer.

$$(VII-B.1) \quad h = z_1 - z_2 = (RT/g)\ln(p_1/p_2) \text{ where:}$$

z_1 and z_2 are the geometric heights at p_1 and p_2,
R = gas constant for dry air, and
g = gravitational constant.

Figure VII-B.1a shows the scatter plot of the GEOS-4 surface pressure versus the observations reported in the NCDC archive for 2004. Figure VII-B.1b shows the agreement with the application of equation 1, using the 2m daily mean temperature with no correction to the GEOS-4 temperatures (e.g. no lapse rate or offset correction). Figure VII-B.1c shows the scatter plot where the GEOS-4 surface pressure and temperature have been corrected for elevation differences. Clearly, adjustment to the GEOS-4 surface pressures using equation 1 results in significant improvements to the estimates of the NCDC station pressures.
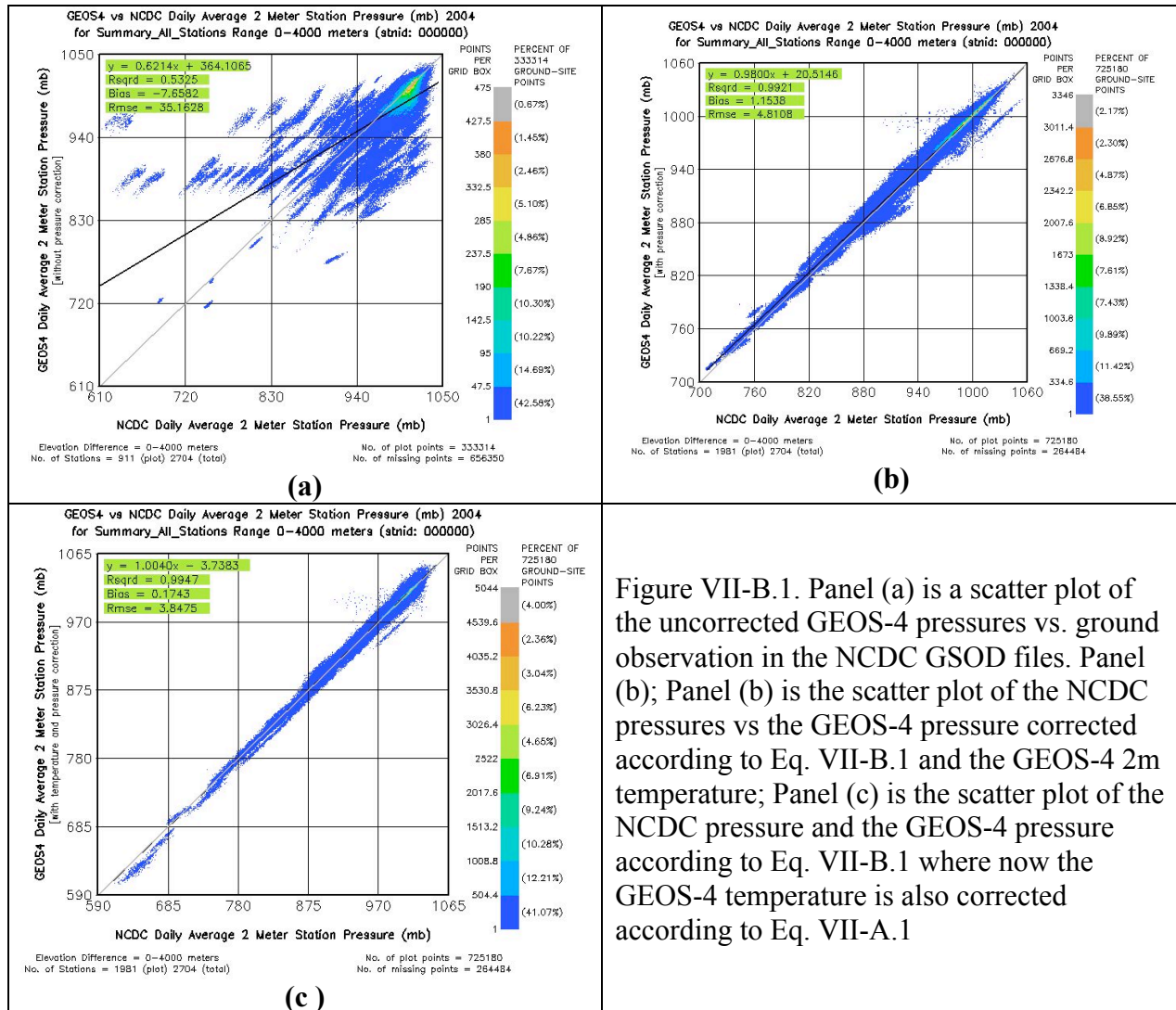
Figure VII-B.1. Panel (a) is a scatter plot of the uncorrected GEOS-4 pressures vs. ground observation in the NCDC GSOD files. Panel (b); Panel (b) is the scatter plot of the NCDC pressures vs the GEOS-4 pressure corrected according to Eq. VII-B.1 and the GEOS-4 2m temperature; Panel (c) is the scatter plot of the NCDC pressure and the GEOS-4 pressure according to Eq. VII-B.1 where now the GEOS-4 temperature is also corrected according to Eq. VII-A.1

(Return to Content)

D. Humidity (Dew Point/Frost Point) [Validation in Progress]
(Return to Content)

E. Precipitation: The precipitation data in SSE Release 6.0 has been obtained from the Global Precipitation Climate Project (GPCP - http://precip.gsfc.nasa.gov). The GPCP precipitation data product, Version 2.1, is a global 2.5°x2.5° monthly accumulation based upon combination of observations from multiple platforms described at http://precip.gsfc.nasa.gov/gpcp_v2.1_comb_new.html . One degree SSE estimates of precipitation are based upon replicating GPCP values for SSE cell that overlap GPCP cells and averaging GPCP values when the SSE cell overlaps two or more GPCP cells. Validation and additional details relative to GPCP Version 2.1 precipitation values can be found in Adler, et. al. 2003.
(Return to Content)

VIII. Wind Speed

The main focus of the wind parameters in SSE Release 6.0 continues to be applications related to power generation via wind. Accordingly, the primary emphasis was place on providing accurate winds at 50 m above the Earth's surface. Based upon analysis of the winds in GEOS-4 relative to winds provided in the previous release of SSE (i.e. Release 5.1), Release 6.0 winds continue to be based on the Version 1 GEOS (GEOS-1) reanalysis data set described in Takacs, Molod, and Wang (1994). In particular, the 50-meter velocities were derived from GEOS-1 surface values using equations provided by GEOS project personnel. Adjustments were made in a few regions based on surface type information from Dorman and Sellers (1989) and recent vegetation maps developed by the International Geosphere and Biosphere Project (IGBP) (Figure VIII-1). GEOS-1 vegetation maps were compared with IGBP vegetation maps. Significant differences in the geographic distribution of crops, grasslands, and savannas were found in a few regions. In those regions, airport data were converted to new 50-m height velocities based on procedures in Gipe (1999). GEOS-1 50-m values were replaced with the Gipe-derived estimates in those regions.

Ten-year annual average maps of 50-m and 10-m "airport" wind speeds are shown in Figure VIII.2. Velocity magnitude changes are now consistent with general vegetation heights that might be expected from the scene types in Figure VIII.1. Note that SSE heights are above the soil, water, or ice surface and not above the "effective" surface in the upper portion of vegetation canopies.
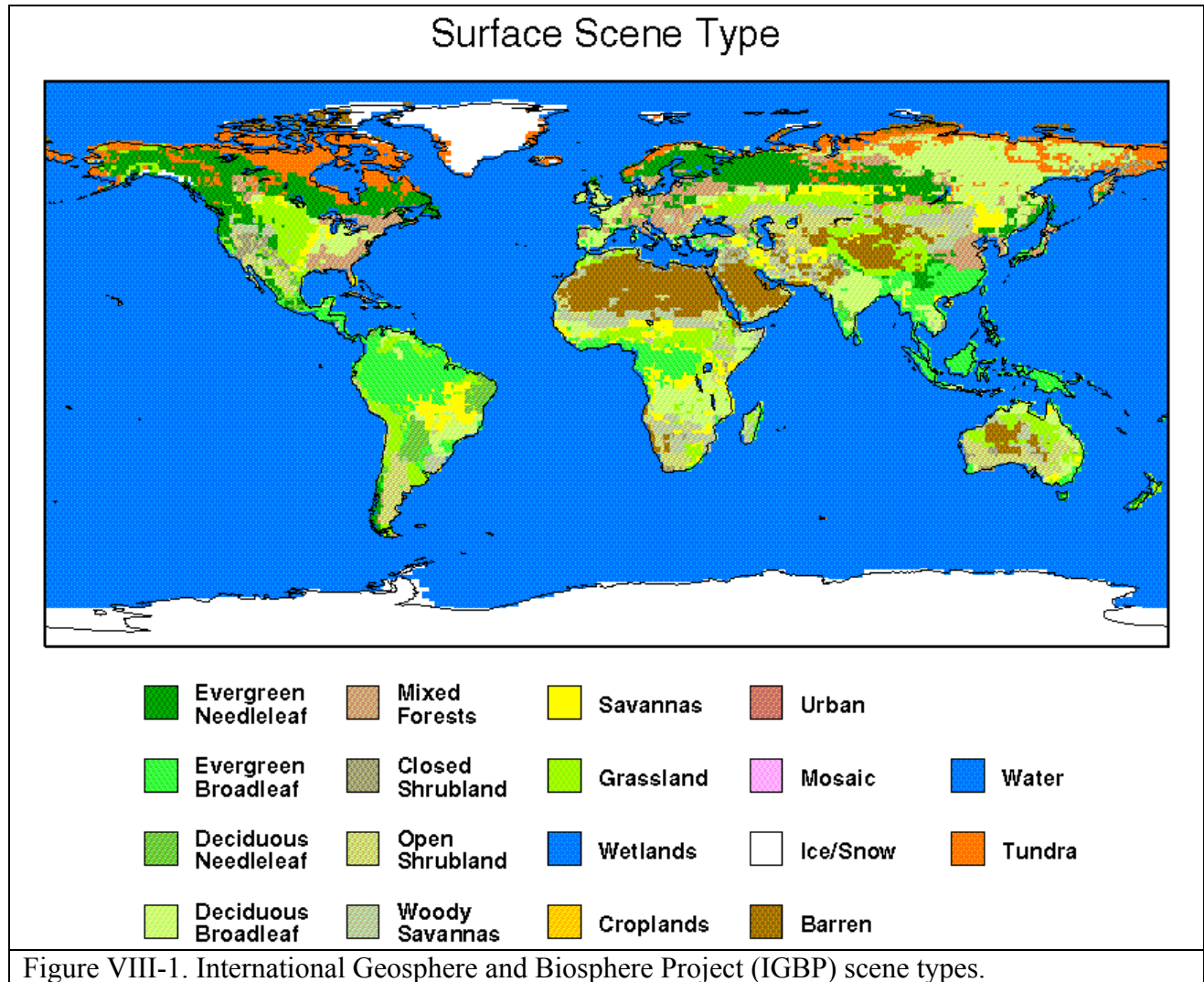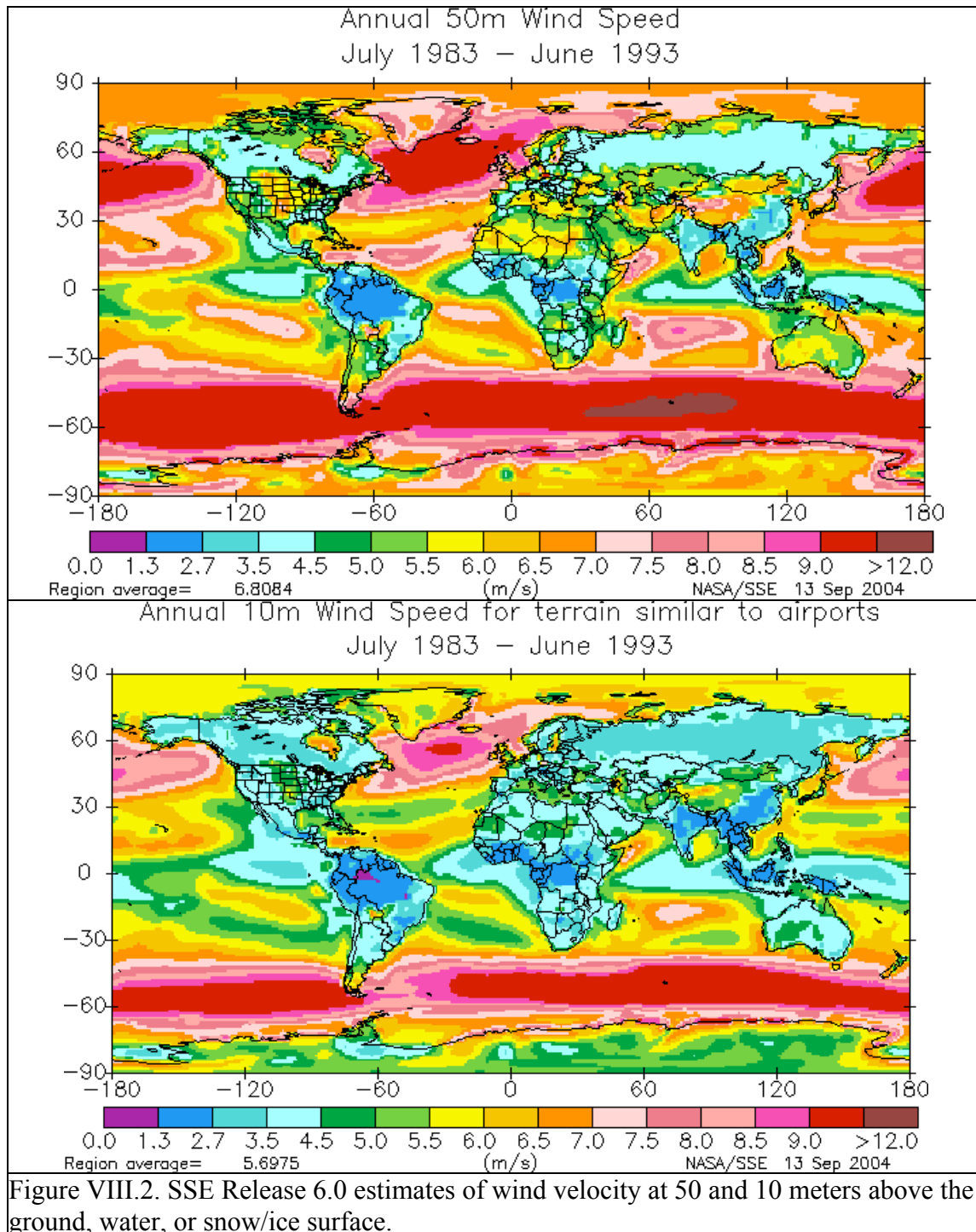
Figure VIII-1. International Geosphere and Biosphere Project (IGBP) scene types.

Ten-year average SSE "airport" estimates were compared with 30-year average airport data sets over the globe furnished by the RETScreen project. In general, monthly bias values varied between ±0.2 m/s and RMS (including bias) values are approximately 1.3 m/s (Fig. VIII.3). This represents a 20 to 25 percent level of uncertainty relative to mean monthly values and is about the same level of uncertainty quoted by Schwartz (1999). Gipe (1999) notes that operational wind measurements are sometimes inaccurate for a variety of reasons. Site-by-site comparisons at nearly 790 locations indicate SSE 10-m "airport" winds tend to be higher than airport measurements in remote desert regions in some foreign countries. SSE values are usually lower than measurements in mountain regions where localized accelerated flow may occur at passes, ridge lines or mountain peaks. One-degree resolution wind data is not an accurate predictor of local conditions in regions with significant topography variation or complex water/land boundaries.

Designers of "small-wind" power sites need to consider the effects of vegetation canopies affecting wind from either some or all directions. Trees and shrub-type vegetation with various

heights and canopy-area ratios reduce near-surface velocities by different amounts. GEOS-1 calculates 10-m velocities for a number of different vegetation types. Values are calculated by parameterizations developed from a number of "within-vegetation" experiments in Canada, Scandinavia, Africa, and South America. The ratio of 10-m to 50-m velocities (V10/V50) for 17 vegetation types is provided in Table VIII.1. All values were taken from GEOS-1 calculations except for the "airport" flat rough grass category that was taken from Gipe.

Figure VIII.2. SSE Release 6.0 estimates of wind velocity at 50 and 10 meters above the ground, water, or snow/ice surface.
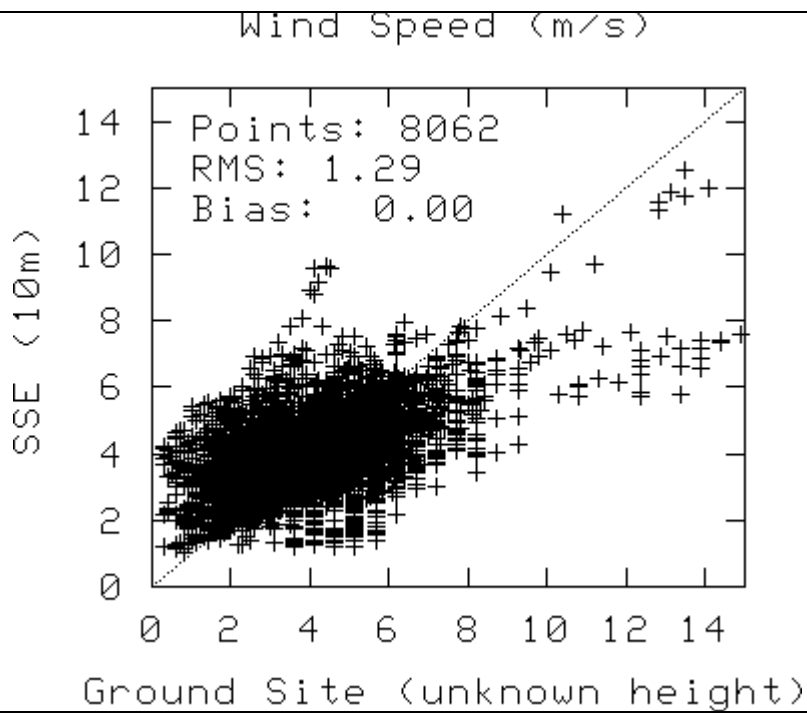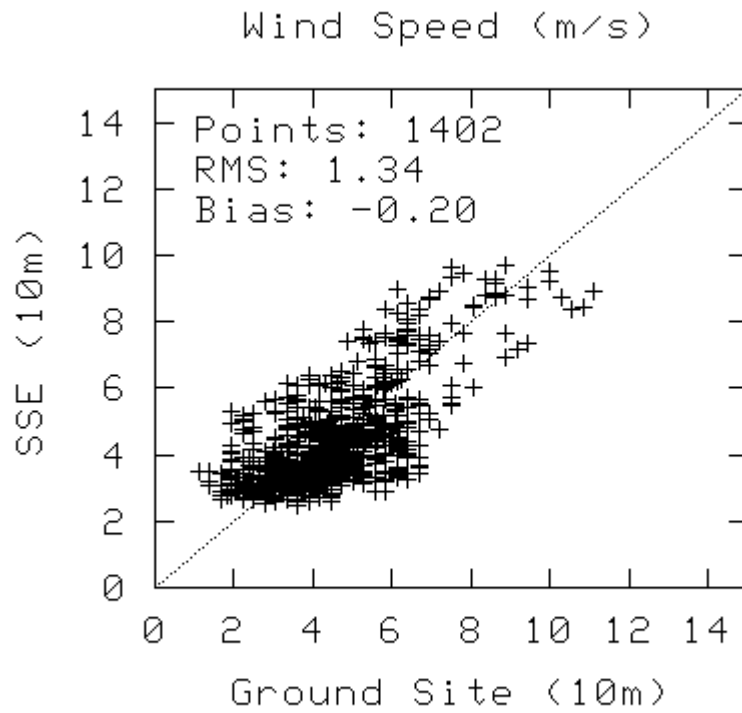
Figure VIII.3. Comparison of monthly means based upon 10-year Release 6 SSE 10-m wind speed with monthly means based upon 30-year RETScreen site data.

Table VIII.1. Wind Velocity V10/V50 Ratio for Various Vegetation Types.												
Northern hemisphere month	1	2	3	4	5	6	7	8	9	10	11	12
35-m broadleaf-evergreen trees (70%) small type	0.47	0.47	0.47	0.47	0.47	0.47	0.47	0.47	0.47	0.47	0.47	0.47
20-m broadleaf-deciduous trees (75%)	0.58	0.57	0.56	0.55	0.53	0.51	0.49	0.51	0.53	0.55	0.56	0.57
20-m broadleaf & needleleaf trees (75%)	0.44	0.47	0.50	0.52	0.53	0.54	0.54	0.52	0.50	0.48	0.46	0.45
17-m needleleaf-evergreen trees (75%)	0.50	0.53	0.56	0.58	0.57	0.56	0.55	0.55	0.55	0.54	0.53	0.52
14-m needleleaf-deciduous trees (50%)	0.52	0.53	0.55	0.57	0.57	0.58	0.58	0.54	0.51	0.49	0.49	0.50
18-m broadleaf trees (30%)/groundcover	0.52	0.52	0.52	0.52	0.52	0.52	0.52	0.52	0.52	0.52	0.52	0.52
0.6-m perennial groundcover (100%)	0.65	0.65	0.65	0.65	0.65	0.65	0.65	0.65	0.65	0.65	0.65	0.65
0.5-m broadleaf (variable %)/groundcover	0.65	0.65	0.65	0.65	0.65	0.65	0.65	0.65	0.65	0.65	0.65	0.65
0.5-m broadleaf shrubs (10%)/bare soil	0.65	0.65	0.65	0.65	0.65	0.65	0.65	0.65	0.65	0.65	0.65	0.65
0.6-m shrubs (variable %)/groundcover	0.65	0.65	0.65	0.65	0.65	0.65	0.65	0.65	0.65	0.65	0.65	0.65
Rough bare soil	0.70	0.70	0.70	0.70	0.70	0.70	0.70	0.70	0.70	0.70	0.70	0.70
Crop: 20-m broadleaf-deciduous trees (10%) & wheat	0.64	0.62	0.69	0.57	0.57	0.57	0.57	0.57	0.57	0.59	0.61	0.63
Rough glacial snow/ice	0.57	0.59	0.62	0.64	0.64	0.64	0.64	0.64	0.62	0.59	0.58	0.57
Smooth sea ice	0.75	0.78	0.83	0.86	0.86	0.86	0.86	0.82	0.78	0.74	0.74	0.74
Open water	0.85	0.85	0.85	0.85	0.85	0.85	0.85	0.85	0.85	0.85	0.85	0.85
"Airport": flat ice/snow	0.85	0.85	0.85	0.85	0.85	0.85	0.85	0.85	0.85	0.85	0.85	0.85
"Airport": flat rough grass	0.79	0.79	0.79	0.79	0.79	0.79	0.79	0.79	0.79	0.79	0.79	0.79

Note: 10-m and 50-m heights are above soil, water, or ice surfaces, not above the "effective" surface near the tops of vegetation.

IX. References

Adler, R.F., G.J. Huffman, A. Chang, R. Ferraro, P. Xie, J. Janowiak, B. Rudolf, U. Schneider, S. Curtis, D. Bolvin, A. Gruber, J. Susskind, P. Arkin, E. Nelkin 2003: The Version 2 Global Precipitation Climatology Project (GPCP) Monthly Precipitation Analysis (1979-Present). *J. Hydrometeor.*, **4**, 1147-1167.

Barry, R. G. and R. J. Chorley, 1987: *Atmosphere, Weather, and Climate.* 5th ed. Methuen, 460 pp.

Blandford, Troy R., Karen S. Blandford, Bruan J. Harshburger, Brandon C. Moore, and Von P. Walden. Seasonal and Synoptic Variations in near-Surface Air Temperature Lapse Rates in a Mountainous Basin. J. Applied Meteorology and Climatology. 2008, Vol. 47, 249 – 261.

Bloom, S., A. da Silva, D. Dee, M. Bosilovich, J.-D. Chern, S. Pawson, S. Schubert, M. Sienkiewicz, I. Stajner, W.-W. Tan, M.-L. Wu, Documentation and Validation of the Goddard

Earth Observing System (GEOS) Data Assimilation System - Version 4, Technical Report Series on Global Modeling and Data Assimilation, NASA/TM—2005–104606, Vol. 26, 2005

Braun, J. E. and J. C. Mitchell, 1983: Solar Geometry for Fixed and Tracking Surfaces. Solar Energy, Vol. 31, No. 5, pp. 439-444.

Briggs, Robert S., R. G. Lucas, Z. T. Taylor, 2003: Climate Classification for Building Energy Codes and Standards. Technical Paper, Pacific NW National Laboratory, March 26, 2002. Continue to use original climate zone definitions.

Collares-Pereira, M. and A. Rabl, 1979: The Average Distribution of Solar Radiation-Correlations Between Diffuse and Hemispherical and Between Daily and Hourly Insolation Values. Solar Energy, Vol. 22, No. 1, pp. 155-164.

Dorman, J. L. and P. J. Sellers, 1989: A Global Climatology of Albedo, Roughness Length and Stomatal Resistance for Atmospheric General Circulation Models as Represented by the Simple Biosphere Model (SiB). Journal of Atmospheric Science, Vol. 28, pp. 833-855.

Erbs, D. G., S. A. Klein, and J. A. Duffie, 1982: Estimation of the Diffuse Radiation Fraction for Hourly, Daily and Monthly average Global Radiation. Solar Energy, Vol. 28, No. 4, pp. 293-302.

Gipe, Paul, 1999: Wind Energy Basics, Chelsea Green Publishing, 122 pp.

Gupta, S. K., D. P. Kratz, P. W. Stackhouse, Jr., and A. C. Wilber, 2001: The Langley Parameterized Shortwave Algorithm (LPSA) for Surface Radiation Budget Studies. NASA/TP-2001-211272, 31 pp.

Harlow, R. C., E. J. Burke, R. L. Scott, W. J. Shuttleworth, C. M. Brown, and J. R. Petti. Derivation of temperature lapse rates in semi-arid southeastern Arizona, (2004) Hydrol. and Earth Systems Sci, 8(6) 1179-1185.

Klein, S.A., 1977: Calculation of monthly average insolation on tilted surfaces. Solar Energy, Vol. 19, pp. 325-329.

Liu, B. Y. H. and R. C. Jordan, 1960: The Interrelationship and Characteristic Distribution of Direct, Diffuse, and Total Solar Radiation. Solar Energy, Vol. 4, No. 3, pp. 1-19.

Lookingbill, Todd R. and Dean L. Urban, Spatial estimation of air temperature differences for landscape-scale studies in mountain environments, (2003) Agri. and Forst. Meteor, 114(3-4) 141-151.

Ohmura, Atsumu, Ellsworth G. Dutton, Bruce Forgan Claus Fröhlich Hans Gilgen, Herman Hegner, Alain Heimo, Gert König-Langlo, Bruce McArthur, Guido Mueller, Rolf Philipona, Rachel Pinker, Charlie H. Whitlock, Klaus Dehne, and Martin Wild, 1998: Baseline Surface

Radiation Network (BSRN/WCRP): New Precision Radiometry for Climate Research, Bull. Of American Meteor. Soc., **79**, 10, p 2115-2136.

RETScreen: Clean Energy Project Analysis: RETScreen® Engineering & Cases Textbook, Third Edition, Minister of Natural Resources Canada, September 2005. (http://www.retscreen.net/ang/12.php, Engineering e-Textbook, Version 4, RETScreen Photovoltaic Project Analysis Chapter, pp. PV.15-PV.21, ISBN: 0-662-35672-1, Catalogue no.: M39-99/2003E-PDF).

Pinker, R., and I. Laszlo, 1992: Modeling Surface Solar Irradiance for Satellite Applications on a Global Scale. *J. Appl. Meteor.,* 31, 194–211.

Schwartz, Marc, 1999: Wind Energy Resource Estimation and Mapping at the National Renewable Energy Laboratory. NREL Conf. Pub. NREL/CP-500-26245.

Smith, G.L., R. N. Green, E. Raschke, L. M. Avis, J. T. Suttles, B. A. Wielicki, and R. Davies, 1986: Inversion methods for satellite studies of the Earth's radiation budget: Development of algorithms for the ERBE mission. Rev. Geophys., 24, 407-421.

Surface Weather Observations and Reports, Federal Meteorological Handbook No. 1, FCM-H1-2005, Washington, D.C., 2005

Rasch, P. J., N. M. Mahowald, and B. E. Eaton (1997), Representations of transport, convection, and the hydrologic cycle in chemical transport models: Implications for the modeling of short-lived and soluble species, J. Geophys. Res., 102(D23), 28, 127-128, 138.

Takacs, L. L., A. Molod, and T. Wang, 1994: Volume 1: Documentation of the Goddard Earth Observing System (GEOS) general circulation model - version 1, NASA Technical Memorandum 104606, Vol. 1, 100 pp.

White, J.W. et al., Evaluation of NASA satellite- and assimilation model-derived long-term daily temperature data over the continental US, Agric. Forest Meteorol. (2008), doi:10.1016/j.agrformet.2008.05.017